Optimization of pyrrolizine-based Schiff bases with 4-thiazolidinone motif: Design, synthesis and investigation of cytotoxicity and anti-inflammatory potency

Ahmed M. Shawky, Mohammed A.S. Abourehab, Ashraf N. Abdalla, Ahmed M. Gouda

PII: S0223-5234(19)30932-8

DOI: https://doi.org/10.1016/j.ejmech.2019.111780

Reference: EJMECH 111780

To appear in: *European Journal of Medicinal Chemistry*

Received Date: 1 September 2019

Revised Date: 4 October 2019

Accepted Date: 9 October 2019

Please cite this article as: A.M. Shawky, M.A.S. Abourehab, A.N. Abdalla, A.M. Gouda, Optimization of pyrrolizine-based Schiff bases with 4-thiazolidinone motif: Design, synthesis and investigation of cytotoxicity and anti-inflammatory potency, *European Journal of Medicinal Chemistry* (2019), doi: https://doi.org/10.1016/j.ejmech.2019.111780.

Optimization of pyrrolizine-based Schiff bases with 4-thiazolidinone motif: design, synthesis and investigation of cytotoxicity and anti-inflammatory potency

Ahmed M Shawky[1], Mohammed A.S. Abourehab[2,3], Ashraf N. Abdalla[4,5], Ahmed M. Gouda[6,7,*]

[1]Science and Technology Unit (STU), Umm Al-Qura University, Makkah 21955, Saudi Arabia;

[2]Department of Pharmaceutics, Faculty of Pharmacy, Umm Al-Qura University, Makkah 21955, Saudi Arabia;

[3]Department of Pharmaceutics, Faculty of Pharmacy, Minia University, Minia 61519, Egypt;

[4]Department of pharmacology, Faculty of Pharmacy, Umm Al-Qura University, Makkah 21955, Saudi Arabia;

[5]Department of Pharmacology, Medicinal and Aromatic plants research institute, National center for research, Khartoum 2404, Sudan.

[6]Department of Pharmaceutical Chemistry, Faculty of Pharmacy, Umm Al-Qura University, Makkah 21955, Saudi Arabia;

[7]Medicinal chemistry department, Faculty of pharmacy, Beni-Suef University, Beni-Suef 62514, Egypt;

***Correspondence: Ahmed M. Gouda:** Department of Medicinal Chemistry, Faculty of Pharmacy, Beni-Suef University, Beni-Suef 62514, Egypt.

Scopus ID: 26321547200

ORCID: 0000-0003-4527-8885

Tel.: (002)-01126897483

Fax: (002)-082-2162133

E-mail address: ahmed.gouda@pharm.bsu.edu.eg or amsaid@uqu.edu.sa

Highlights

1- Two new series of pyrrolizines bearing Schiff bases or 4-thiazolidinone moiety were synthesized.

2- Compound **12** displayed potent cytotoxic activity (IC_{50} = 0.10 µM) against MCF-7 cells.

3- Compound **22** induced G1 cell cycle arrest and apoptosis in MCF-7 cells.

4- Compounds **12**, **19** and **22** displayed inhibitory activity against CDK2 (IC_{50} = 0.58-1.27 µM).

5- Compounds **14** exhibited potent *in vivo* anti-inflammatory activity mediated by COX-2 inhibition (IC_{50} = 0.64 µM).

6- Binding modes of the new compounds into COXs, CDK2, Aurora A, BRAF and EGFR enzymes were investigated.

Graphical abstract

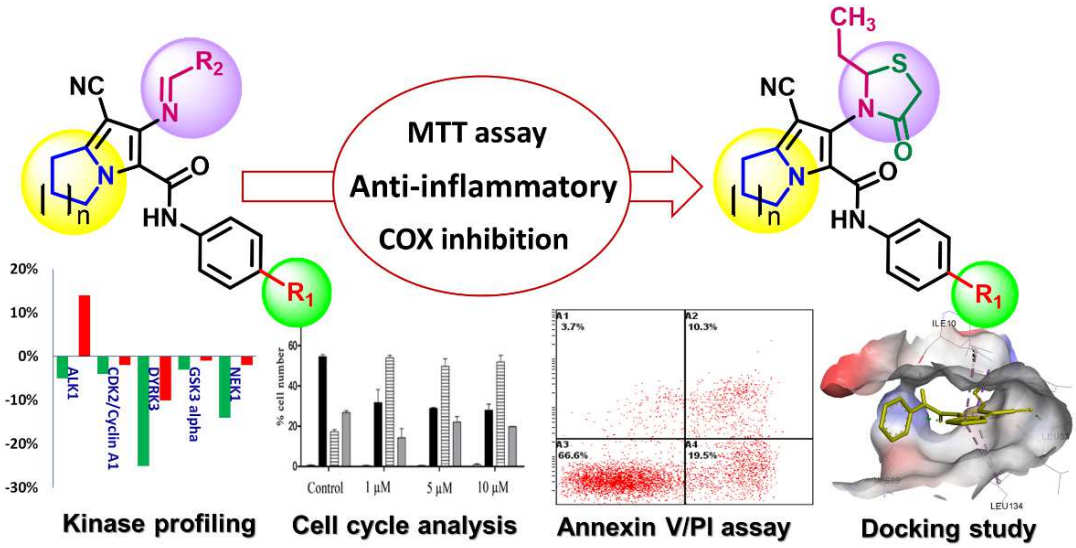

Key words:

Pyrrolizine; cytotoxicity; COX; Kinase; Apoptosis; Cell cycle analysis.

Abstract

Two new series of pyrrolizine-5-carboxamides were synthesized and evaluated for their anticancer and anti-inflammatory activities. The new compounds exhibited potent cytotoxicity (IC_{50} = 0.10-22.96 µM) against three cancer (MCF-7, A2780 and HT29) cell lines with selectivity index in the range of 1-258. Moreover, these compounds also exhibited significant anti-inflammatory activity (18.13-44.51% inhibition of inflammation) mediated by inhibition of COX-1/2 with preferential inhibition of COX-2. The study of SAR revealed favorable cytotoxic outcomes of the aliphatic side chain and 4-thiazolidinone moiety at C6 of the pyrrolizine nucleus, while anti-inflammatory activities was improved with the (hetero)aromatic substituents. The IC_{50} values which inhibit COX-2 were higher than those needed to inhibit the growth of cancer cell lines. Mechanistic studies also revealed inhibition of multiple kinases by compounds **12**, **19** and **22**. Moreover, compounds **12**, **14**, **16** and **22** induced cell cycle arrest and apoptosis in MCF-7 cells. Docking studies revealed nice fitting of the new compounds into COX-1/2. Additionally, compounds **12**, **19** and **22** also exhibited higher affinity for CDK2 than CAN508. To sum up, the above-mentioned data highlight these compounds as promising anti-inflammatory and anticancer agents.

1. Introduction

Combination therapy represents the cornerstone in the treatment of complex diseases [1]. The high efficacy of combination compared to cancer monotherapy is due to simultaneous targeting of multiple enzymes or signaling pathways involved in cancer [2,3]. However, the wide use of combined drugs was restricted by some limitations including the high cost, drug toxicity and interactions [1,3,4]. These problems can be solved with the use of multi-target anticancer agents [5]. A single multi-targeted agent can be used to avoid the pharmacokinetic and drug interaction problems associated with combination therapy [5,6]. Several multi-targeted agents are used effectively in treatment of cancers [7]. However, acquired resistance was also developed for these drugs [8,9].

NSAIDs are commonly in management of cancer-related inflammation and pain [10]. Moreover, their chemopreventive effect attracted much attention in the last two decades. The relationship between inflammation and cancer was also discussed in many reports [12,13]. The upregulation of cyclooxygenase 2 (COX-2) gen was confirmed in different types of solid tumors [14,15]. Accordingly, targeting COX-2 enzyme could provide a new approach in cancer prevention and therapy. This approach was supported by the high anticancer activity of some selective COX-2 inhibitors [16]. Moreover, other types of COXs inhibitors also exhibited anticancer activity against diverse types of cancer cells [17]. However, the exact mechanism of anticancer activity of COXs inhibitors is still unclear [16]. In addition, their use in prevention and treatment of cancers was restricted by many dangerous side effects [18].

Recently, the diarylpyrrolizine derivatives were in our focus as potential therapeutic agents with polypharmacological profile. Among these derivatives, licofelone **1** and compound **2** (**Fig. 1**) displayed both anti-inflammatory and anticancer activities [19-22]. The anticancer activity of compounds **1** and **2** was mediated by induction of apoptosis in colon (HCA-7) and breast (MCF-7) cancer cells, respectively [21,22]. Although licofelone **1** has dual COX/lipoxygenase (LOX) inhibitory activity, the induction of apoptosis in HCA-7 cells was mediated by inhibition of the epidermal growth factor receptor (EGFR) and its downstream kinases [22], which was mediated by decrease in cell membrane fluidity rather than direct inhibition of the enzyme.

Combination of licofelone **1** with several anticancer agents enhanced their anticancer efficacy against different types of cancers [23-25]. Specifically, combining licofelone with the EGFR

inhibitor gefitinib showed synergistic growth and progress suppression of pancreatic carcinoma in mice [25]. Similar results were also observed when erlotinib was combined with selective/nonselective COX inhibitors [26-28].

Rational design

The rational design of multi-target agents can be achieved by incorporating two or more pharmacophores into one scaffold [29-30], which can target different enzymes/pathways. Encouraged by these findings, we have designed two new scaffolds (A and B) to target both oncogenic protein kinases (PKs) and COX enzymes, simultaneously. The first scaffold A (**Fig. 1**) was designed by incorporating the pharmacophoric features of the COX inhibitor licofelone **1** and those of the tyrosine kinase inhibitor CGP-59326 **3** [31]. Structure activity relationship (SAR) of both licofelone **1** and CGP-59326 **3** was considered in the design of scaffold A. Structural modifications of scaffold A included expansion of the pyrrolidine ring (n = 1, 2) and variation of the side chain at C6 to include aliphatic, aromatic or heteroaromatic moieties, **Fig. 1**.

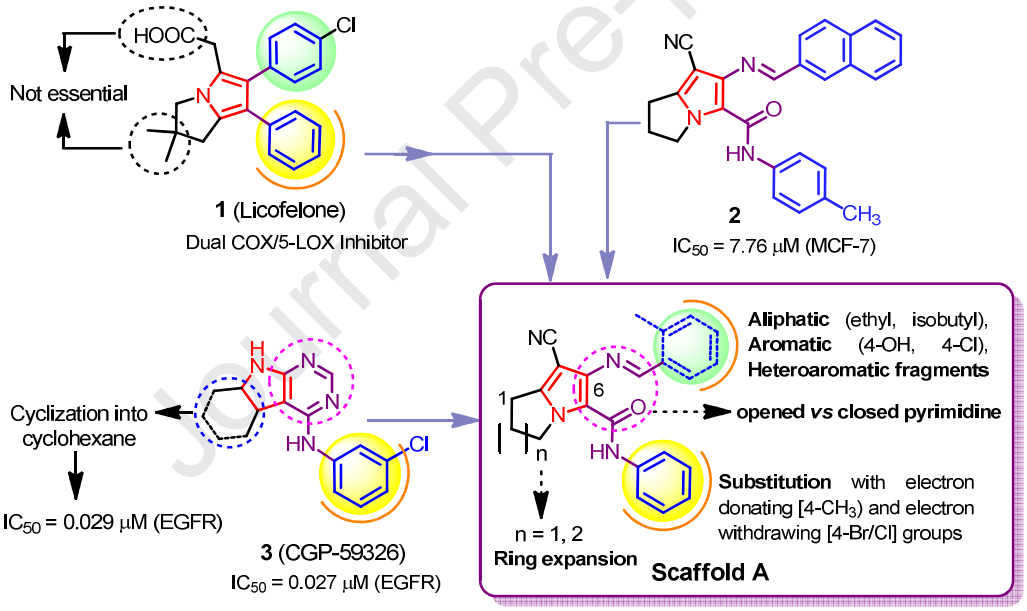

Fig. 1. Rational design and structural modifications of scaffold A.

Moreover, several mono/disubstituted 4-thiazolidinone-based derivatives (**Fig. 2**) exhibited potent anticancer activity with IC_{50} values in the nanomolar rang [32-37]. Mechanistic studies of these compounds revealed inhibition of diverse oncogenic kinases. Among these derivatives, compounds **4** and **5** displayed potent inhibition of cyclin dependent kinase 2 (CDK2) and aurora A kinase, respectively [32,34]. In another attempt to target both oncogenic protein kinases (PKs) and COX enzymes, simultaneously, we have designed scaffold B by incorporating the 4-thiazolidinone ring and scaffold A. The SAR of scaffold B

was studied by variation of substituents on phenyl ring and expansion of pyrrolidine ring (n = 2), **Fig. 2**.

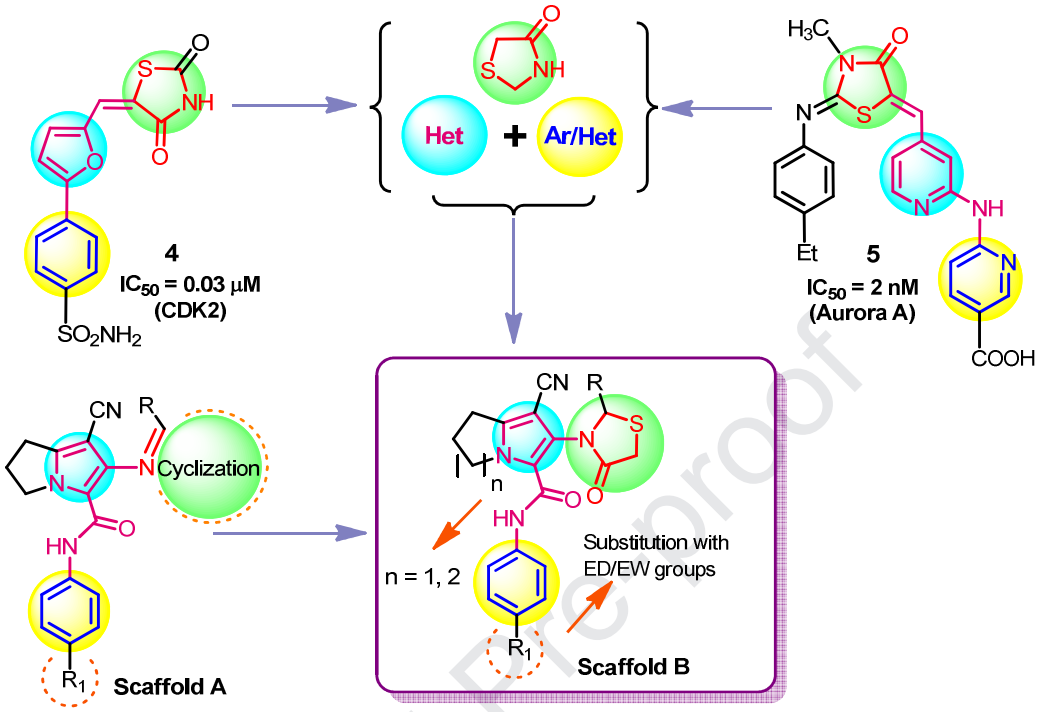

Fig. 2. Rational design and structural modifications of scaffold B.

2. Results and discussion

2.1. Chemistry

Preparation of compounds **7**, **9a-d** and **10a-d** was described in **Scheme 1**, following the previous reports [38-41]. The starting materials **10a-d** were selected out of 28 pyrrolizine derivatives bearing substituents with different sigma (σ) constants on the phenyl ring. Initially, the 28 pyrrolizine underwent preliminary evaluation of their binding affinity to COXs, synthetic accessibility and drugs-likeness scores (Table S1 and S2, supplementary data). In this study, compounds **10a-d** showed considerable affinity for COX-1/2. Considering the structural differences between the active site of COX-2 and COX-1 [42], it is expected that affinity of the new compounds **11-18** to COX-2 will be optimized with the increase in their molecular volume as compared to the starting materials. Compounds **11-18** were obtained by condensation of the pyrrolizine-5-carboxamide derivatives **10a** with the appropriate aldehydes in ethanol, **Scheme 1**. The new compounds were obtained in good yield (61-75%), **Table 1**.

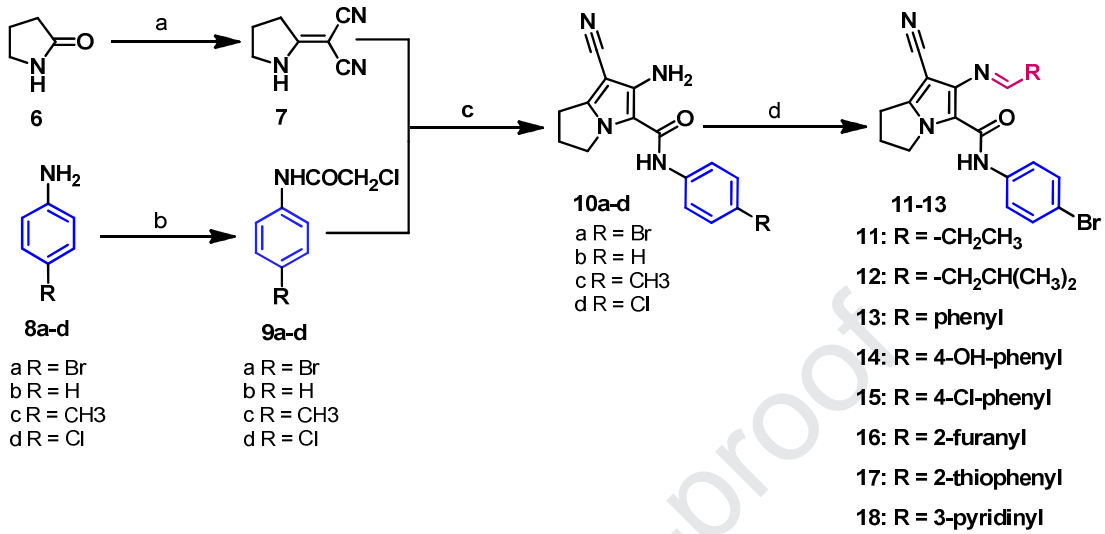

Scheme 1. Reagents and reaction conditions: (a) $(CH_3)_2SO_4$, benzene, $CH_2(CN)_2$; (b) $ClCH_2COCl$, gl. AcOH, CH_3COONa; (c) acetone, K_2CO_3, reflux, 24 h; (d) appropriate aldehyde, EtOH, gl. AcOH, stir 2h at 40-50 °C, reflux, 6 h.

Table 1. Melting points and yield% of compounds **11-24**, **28** and **29**.

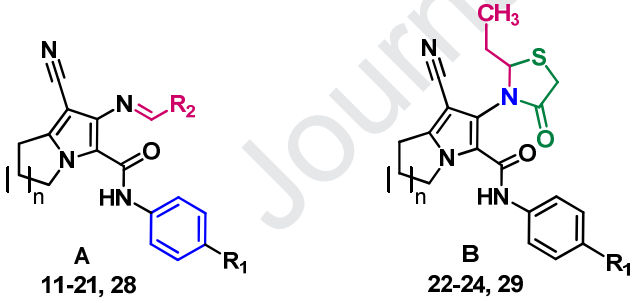

Comp. No	Scaffold	R_1	R_2	n	m.p. (°C)	Yield%
11	A	Br	C_2H_5	1	227-9	61%
12	A	Br	$CH_2CH(CH_3)_2$	1	207-9	64%
13	A	Br	C_6H_5	1	265-7	71%
14	A	Br	4-OH-C_6H_4	1	320-2	73%
15	A	Br	4-Cl-C_6H_4	1	285-7	75%
16	A	Br	2-furanyl	1	261-3	69%
17	A	Br	2-thiophenyl	1	250-2	65%
18	A	Br	3-pyridinyl	1	271-3	71%
19	A	H	C_2H_5	1	212-4	65%
20	A	CH_3	C_2H_5	1	217-9	59%
21	A	Cl	C_2H_5	1	226-9	71%
22	B	H	-	1	228-9	58%
23	B	CH_3	-	1	237-40	63%

24	B	Cl	-	1	249-51	68%
28	A	H	C_2H_5	2	209-11	54%
29	B	H	-	2	228-31	56%

To optimize activity of the new compounds, a preliminary evaluation of their cytotoxic activity was performed. The 3-(4,5-dimethylthiazol-2-yl)-2,5-diphenyl-2H-tetrazolium bromide (MTT) assay was used in this evaluation according to the previous report [43]. In this evaluation, MCF-7 breast cancer cell line was selected representing the leading cancer in incidence and mortality among women [44]. Cancer cells were treated with single dose (5 µM) of the eight compounds **11-18** and growth% was determined after 48 h. Results were represented in **Fig. 3**.

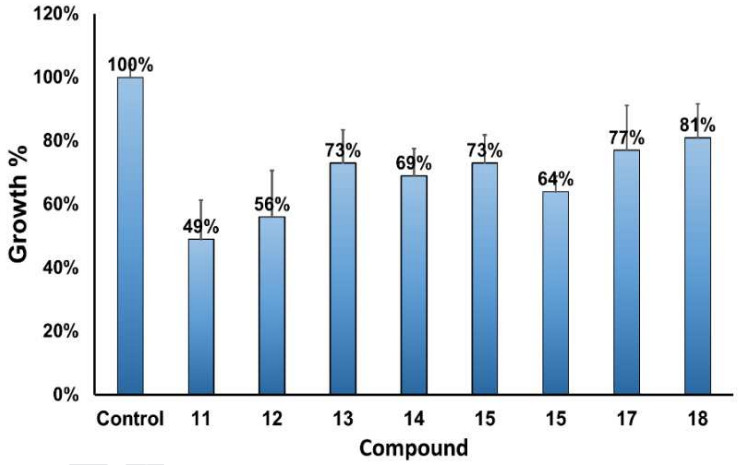

Fig. 3. Growth% of MCF-7 cells after single-dose treatment with compounds **11-18** (5 µM) for 48 h, results were presented as mean ± S.D. (n = 6).

Results of the preliminary cytotoxic evaluation revealed the highest growth inhibitory activity for compounds **11** and **12** which have aliphatic side chain at C6. Compounds **13-15**, with the aromatic rings in the side chain at C6, were slightly more active in inhibiting the growth of MCF-7 cells compared to compounds **16-18** with the heteroaromatic rings. Among the eight derivatives, compound **18** was the least active, while compound **11** displayed the highest cytotoxicity. Based on these results (**Fig. 3)**, three new derivatives **19-21** bearing the aliphatic propylideneamino moiety at C6 were prepared by condensation of compounds **10b-d** with propionaldehyde in absolute ethanol, **Scheme 2**. Moreover, three 4-thiazolidinone-bearing derivatives **22-24** were obtained from the reaction of compounds **10b-d** with

propionaldehyde and mercaptoacetic acid. The yield% of these compounds was presented in **Table 1**.

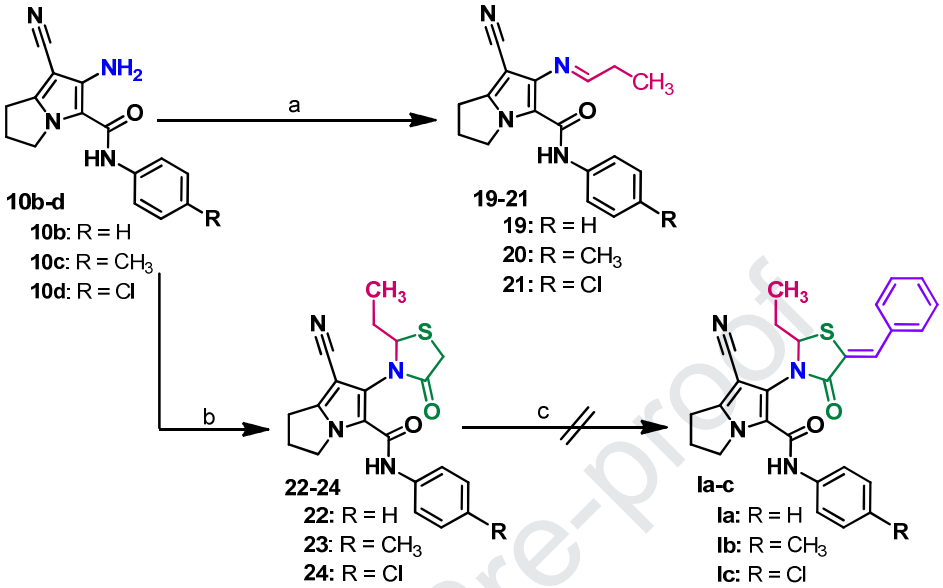

Scheme 2. Reagents and reaction conditions: (a) propionaldehyde, EtOH, gl. AcOH, stir, 2h at 40-50 °C, reflux, 6 h; (b) propionaldehyde, mercaptoacetic acid, DCC, THF, 0 °C; (c) benzaldehyde, gl. AcOH, Na acetate, reflux, 12 h.

Compounds **22-24** were also refluxed with benzaldehyde to afford the condensed product **Ia-c**, **Scheme 2**. Unfortunately, the expected products **Ia-c** were not formed.

Moreover, compound **10a** was allowed to react with aromatic/heteroaromatic aldehydes in order to prepare a new series of 2-(hetero)aryl-thiazolidin-4-one derivatives **IIa-f**, **Scheme 3**. But also this reaction failed to produce the expected compounds **IIa-f**. This could be attributed to the steric hinderance of the bulky (hetero)aromatic moieties. This was also in concordance with the synthetic accessibility scores calculated for these compounds using SwissADME (developed by the Swiss Institute of Bioinformatics, http://www.swissadme.ch/). The scores calculated for compounds **IIa-f** (Table S3, supplementary data) were higher than that of compound **22**.

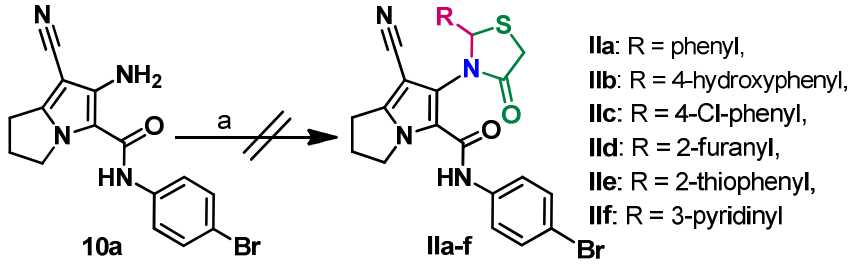

Scheme 3. Reagents and reaction conditions: (a) Ar-CHO (benzaldehyde, 4-hydroxy/chloro-benzaldehyde, furan-2-carbaldehyde, thiophene-2-carbaldehyde, 3-pyridinecarbox-aldehyde), mercaptoacetic acid, DCC, THF, 0 °C.

Synthesis of the tetrahydroindolizines **28** and **29** was described in **Scheme 4**. The starting materials **26** and **27** were synthesized according to the previous reports [40,45]. Compound **27** was reacted with propionaldehyde to afford the Schiff base **28**, while compound **29** was obtained from the reaction of compound **27** with propionaldehyde and mercaptoacetic acid. The yield% of these compounds was presented in **Table 1**.

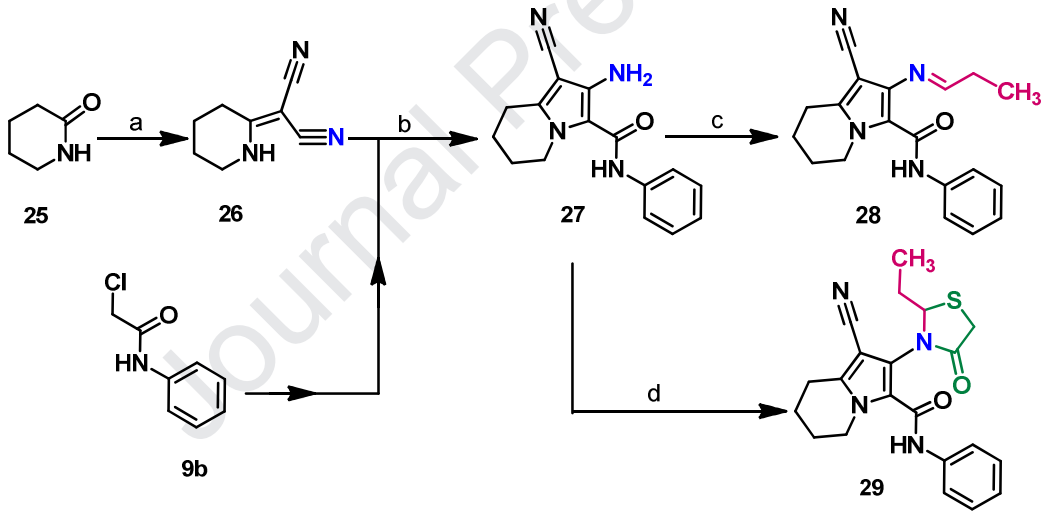

Scheme 4. Reagents and reaction conditions: (a) $(CH_3)_2SO_4$, benzene, $CH_2(CN)_2$; (b) acetone, K_2CO_3, reflux, 24 h; (c) propionaldehyde, EtOH, gl. AcOH, stir 2h at 40-50 °C, reflux, 6 h; (d) propionaldehyde, mercaptoacetic acid, DCC, THF, 0 °C.

2.2. Biological evaluation

2.2.1. Cytotoxic activity

2.2.1.1. Cytotoxicity assay

To evaluate growth inhibitory activity of compounds **11-24**, **28**, **29** and lapatinib as reference drug, MTT assay was used according to our previous report [43]. In this assay, three human

cancer cell lines (breast MCF-7, ovarian A2780 and colon HT29) were used. The results of the treatments with compounds **11-18** for 72h were summarized as IC_{50} values in **Table 2**.

The new compounds **11-18** displayed potent to moderate cytotoxic activity against the three cancer cell lines with IC_{50} values in the range of 0.1-22.96 µM. Among these derivatives, compounds **11** and **12** exhibited the highest cytotoxic activity (IC_{50} = 0.10-0.89 µM). Compound **12** was slightly more active than compound **11** against both MCF-7 and HT29 cancer cell lines, while compound **11** exhibited higher activity against ovarian A2780 cells. The two compounds were also more potent compared to the reference lapatinib (IC_{50} = 6.80-12.67 µM) against the three cancer cell lines, **Table 2**.

Compounds **13-15** displayed potent to moderate cytotoxic activity against the three tested cancer cell lines with IC_{50} values in the range of 0.47-14.48 µM. Among these three derivatives, the 4-hydroxyphenyl analog **14** was the most active against MCF-7 and A2780 cancer cells, **Table 2**..

Table 2. Cytotoxic activity of compounds **11-18**, and lapatinib against MCF-7, A2780, HT29 and MRC5 cell lines.

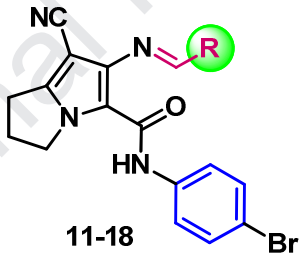

11-18

Comp. No	R	IC_{50} (µM)[a,b]			
		MCF-7	**A2780**	**HT29**	**MRC5**
11	$-CH_2CH_3$	0.14±0.01	0.27±0.08	0.89±0.01	21.25±0.40
12	$-CH_2CH(CH_3)_2$	0.10±0.05	0.52±0.02	0.67±0.33	25.81±0.73
13	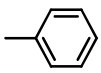	0.50±0.15	4.16±1.27	2.97±0.14	9.00±0.13
14	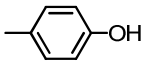	0.49±0.02	0.47±0.04	14.48±4.44	25.03±0.31
15	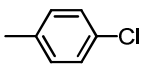	6.03±3.35	8.30±2.02	7.79±1.84	13.85±1.04
16	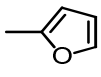	6.89±2.84	12.23±1.27	2.04±0.58	15.68±0.40
17	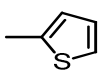	9.41±1.82	19.30±2.13	3.65±0.79	23.10±2.03

18	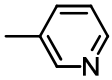	11.29±1.54	22.96±4.17	2.63±0.35	25.56±2.86
Lapatinib	-	6.80± 1.20	10.40± 0.80	12.67±1.33	13.66±2.90

[a] IC_{50} is the concentration of test compound which reduce cellular growth to 50% after treatment for 72 h.
[b] Results represent mean IC_{50} value ± S.D. (n = 3).

Compounds **16-18** with the heteroaromatic rings in the side chain at C6 were less active against both MCF-7 and A2780 cancer cell lines than compounds **13-15**, meanwhile, they were more active against HT29 cells (IC_{50} = 2.04-3.65 µM), **Table 2**.

Cytotoxic activity of the four propylideneamino-bearing derivatives **19-21** and **28** expressed as IC_{50} values were presented in **Table 3**. The four compounds showed potent to moderate cytotoxic activity (IC_{50} = 0.14-15.60 µM) against the three-cancer cell lines. Compound **19** was the most active against MCF-7 cells, while compounds **21** and **28** were the most active against A2780 and HT29 cells, respectively.

Table 3. Cytotoxic activity of compounds **19-21**, **28** and lapatinib against MCF-7, A2780, HT29 and MRC5 cell lines.

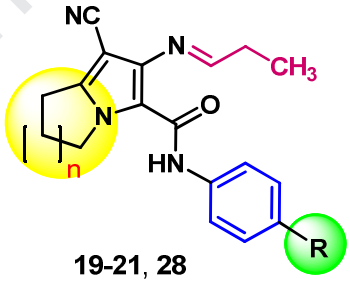

19-21, **28**

Comp. No	R	n	IC_{50} (µM)[a,b]			
			MCF-7	A2780	HT29	MRC5
19	H	1	0.57±0.06	15.60±0.99	0.20±0.01	3.17±0.23
20	CH_3	1	0.84±0.14	3.88±1.08	0.61±0.08	0.56±0.01
21	Cl	1	0.74±0.04	0.58±0.08	1.02±0.06	0.17±0.02
28	H	2	1.43±0.37	15.56±5.64	0.14±0.01	1.53±0.16
Lapatinib	-	-	6.80± 1.20	10.40± 0.80	12.67±1.33	13.66±2.90

[a] IC_{50} is the concentration of test compound which reduce cellular growth to 50% after treatment for 72 h.
[b] Results represent mean IC_{50} value ± S.D. (n = 3).

Among the three cancer cell lines, HT29 was the most sensitive to the four compounds **19**-**21** and **28**, **Table 3**. On the other hand, A2780 cells was the least sensitive to these compounds. The three pyrrolizines **19**-**21** displayed higher activity against the MCF-7 cells compared to the tetrahydroindolizine **28**. Moreover, compound **19** was more active against the three cancer cell lines compared to its corresponding analog **28**.

The 4-thiazolidinone-bearing compounds **22**-**24** and **29** were also evaluated for their cytotoxicity by the MTT assay. The results revealed potent cytotoxic activity with IC_{50} values in the range of 0.11-4.24 µM, against the three cancer cell lines, **Table 4**. It was clear that these compounds have better cytotoxic activity profile compared to their opened analogs **19**-**21** and **28**. Among the four thiazolidinone-bearing derivatives, compound **22** exhibited the highest cytotoxic activity against MCF-7 cells, while compound **23** was the most active against both A2780 and HT29 cells.

Table 4. Cytotoxic activity of compounds **22**-**24**, **29** and lapatinib against MCF-7, A2780, HT29 and MRC5 cell lines.

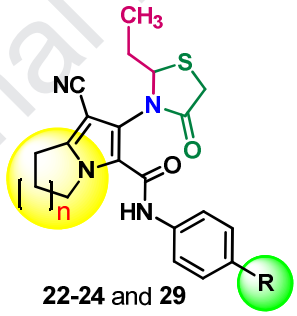

22-24 and **29**

Comp. No	R	n	IC_{50} (µM)[a,b]			
			MCF-7	A2780	HT29	MRC5
22	H	1	0.16±0.08	0.22±0.07	0.60±0.10	0.63±0.09
23	CH_3	1	0.47±0.52	0.11±0.01	0.12±0.03	1.70±0.78
24	Cl	1	0.21±0.04	0.31±0.06	0.20±0.01	0.91±0.10
29	H	2	0.84±0.03	4.24±0.75	2.06±0.07	11.10±0.62
Lapatinib	-	-	6.80± 1.20	10.40± 0.80	12.67±1.33	13.66±2.90

[a] IC_{50} is the concentration of test compound which reduce cellular growth to 50% after treatment for 72 h.
[b] Results represent mean IC_{50} value ± S.D. (n = 3).

2.2.1.2. Evaluation of cytotoxic selectivity

Selectivity toward cancerous cells is one of the major problems which usually appear during the discovery and development of new anticancer agents. To assess the selectivity of our newly synthesized compounds, their cytotoxic activity was evaluated against normal human foetal lung fibroblast (MRC5). MTT assay was used in this evaluation and results were expressed as IC_{50} values, **Tables 2-4**.

Compounds **11**, **12**, **14-18** displayed IC_{50} values in the range of 13.85-25.81 µM against normal MRC5 cells, indicating less toxicity compared with lapatinib (IC_{50} values = 13.66 µM). Among these compounds, compound **12** was the least toxic for the normal MRC5 cells, **Table 2**.

Selectivity index (SI) of the new compounds was calculated to compare their cytotoxic selectivity. The value of SI of each compound was obtained by dividing IC_{50} value of the compound against the normal MRC5, by IC_{50} value of this compounds against the specific cancer cell line.

The Schiff bases **11-18** showed SIs in the range of 1-258, **Fig. 4**. Among these, compounds **11** and **12** displayed the highest cytotoxic selectivity. Compound **11** was 24-152 times more selective for the three cancer cell lines. Moreover, compound **12** was the most selective, showing SI in the range of 39-258 toward the three cancer cell lines.

Compounds **13-15** (with the aromatic rings at C6) exhibited SI of 2-52 for the three cancer cell lines, being less selective than the aliphatic analogs **11** and **12**. On the other hand, compounds **16-18** were the least selective (SI = 1-10) among the eight pyrrolizines **11-18**. Except for compound **16**, all other compounds were more selective than lapatinib for the three cancer cell lines, **Fig. 4**.

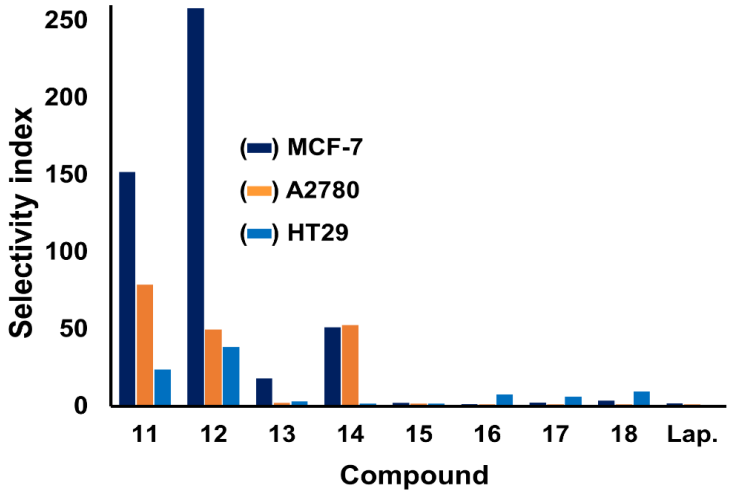

Fig. 4. Selectively index of compounds **11-18** and lapatinib for MCF-7, A2780 and HT29 cancer cells.

Compounds **19-24**, **28** and **29** were also evaluated for their selectivity against MRC5 cells using MTT assay. Compounds **19-24**, **28** and **29** displayed IC_{50} values in the range of 0.17-11.1 µM against the normal MRC5 cells. Among these, the tetrahydroindolizine **29** was the least toxic toward MRC5 cells, **Tables 3** and **4**.

The SIs of compounds **19-24**, **28** and **29** toward the three cancer cell lines was outlined in **Fig. 5**. Generally, the 4-thiazolidinone-bearing derivatives **22-24** and **29** displayed SIs in the range of 3-15 toward MCF-7 and A2780 cells. They were more selective compared to their opened analogs **19-21** and **28**. Among these, compounds **19**, **23** and **29** exhibited the highest selectivity toward HT29, A2780 and MCF-7 cells, respectively.

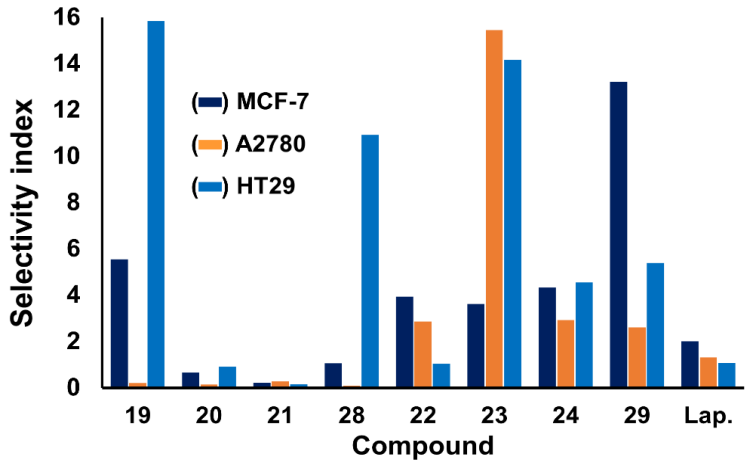

Fig. 5. Selectively index of compounds **19-24**, **28**, **29** and lapatinib for MCF-7, A2780 and HT29 cancer cells.

2.2.1.3. Structure activity relationship (SAR)

The SAR of cytotoxic activity of compounds **11-18**, **19-21** and **28** was outlined in **Fig. 6**. Compounds **11** and **12** with the aliphatic side chain (R_2 = ethyl, isobutyl) were the most active as cytotoxic agents against the three (MCF-7, A2780 and HT29) cancer cell lines. Replacement of bromo (Br) in compound **11** by H, electron donating (CH_3) or electron withdrawing (Cl) groups resulted in a strong drop in cytotoxic activity against A2780 cells. Replacement of the aliphatic side chain (R_2) in compounds **11** and **12** with (hetero)aromatic (phenyl, 4-(hydroxy/chloro)phenyl, 2-furanyl, 2-thiophenyl or 3-pyridinyl) rings resulted in decrease in

cytotoxicity against the three cancer cell lines. In addition, expansion of the pyrrolidine ring in compound **19** to piperidine decreased the cytotoxic activity by nearly ~50%.

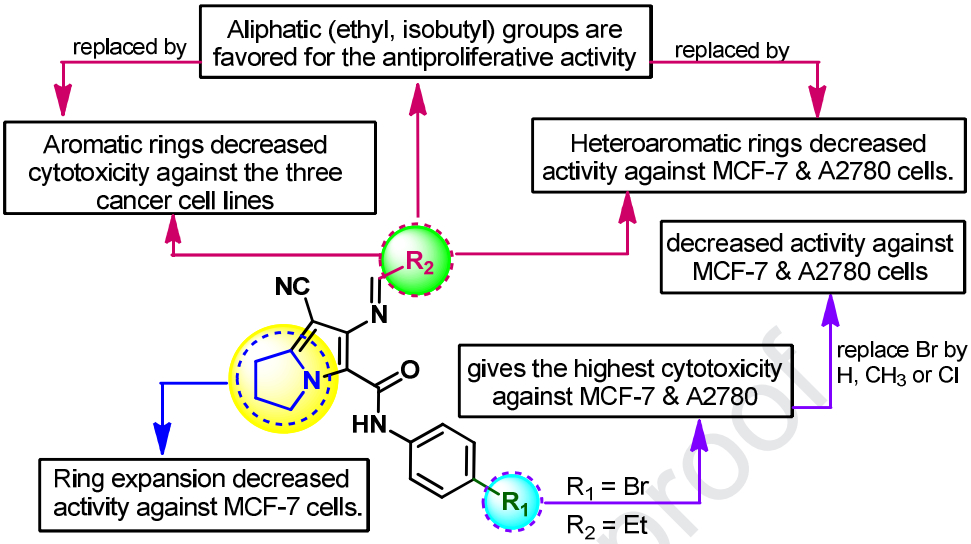

Fig. 6. SAR of cytotoxicity of compounds **11-21** and **28** against MCF-7, A2780 and HT29 cells.

The SAR study of compounds **22-24** and **29** was presented in **Fig. 7**. Cyclization of the propylideneamino side chains in compounds **19-21** and **28** into 4-thiazolidinone ring resulted in improvement of cytotoxicity against both MCF-7 and A2780 cells. Cytotoxicity of compound **22** against HT29 cells was also improved with the 4-methyl (+σ) and 4-chloro (-σ) substituents. On the other hand, expansion of the pyrrolidine ring in compound **22** to piperidine resulted in a noticeable decrease in cytotoxicity against the three cancer cell lines.

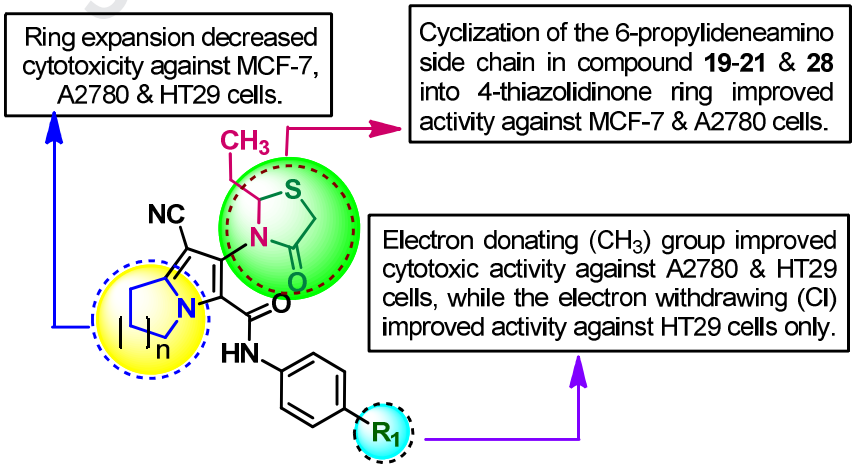

Fig. 7. SAR of cytotoxicity activity of compounds **22-24** and **29** against MCF-7, A2780 and HT29 cells.

2.2.2. Anti-inflammatory activity

2.2.2.1. *In vitro* COX inhibitory activity

Licofelone **1** displayed *in vivo* anti-inflammatory activity mediated at least partially by inhibition of COXs enzymes. In this work, our compounds **11-24**, **28** and **29** were evaluated for their *in vitro* inhibitory activity against COXs using COX inhibitor screening assay kit according to the previous report [46]. The results were presented as IC_{50} values, **Table 5**.

In general, most of the new compounds inhibited the two COXs with preferential inhibition of COX-2. Compounds **11-24**, **28** and **29** displayed IC_{50} values in the range of 0.64-56.1 μM against COX-2. Among these, compound **14** was the most potent as COX-2 inhibitor, while compound **16** was the most active inhibitor of COX-1. Compounds **11** and **29** displayed nearly equal inhibitory activity against the two COXs (SI = ~1). Although compounds **11** and **12** have nearly equal IC_{50} values against COX-2 activity, but compound **12** was more selective toward COX-2, **Table 5**.

Table 5. COX inhibitory activity of compounds **11-24**, **28**, **29**, celecoxib and indomethacin.

	IC_{50} (μM) [a]		**SI** [b]
Comp. No	COX-1	COX-2	
11	14.15±0.85	13.31±0.77	1.06
12	>100	13.49±0.63	>7
13	>100	1.49±0.05	>67
14	71.97±2.9	0.64±0.02	112.45
15	>100	7.53±0.34	>13
16	13.16±0.64	1.65±0.04	7.98
17	>100	9.25±0.44	>10
18	>100	9.84±0.39	>10
19	>100	52.97±2.71	>1.89
20	27.69±1.95	10.33±0.73	2.68
21	15.62±0.71	4.24±0.11	3.68
22	43.72±2.9	10.79±0.67	4.05
23	>100	1.25±0.03	>80
24	>100	1.15±0.02	>86
28	27.22±2.1	7.14±0.25	3.81
29	65.39±3.61	56.10±2.82	1.17
Celecoxib	27.83±14.2	0.25±0.12	111.32
Indomethacin	1.56±0.03	68.45±4.1	0.02

[a] Values represent the mean of four determinations ± SEM, (n = 3).
[b] selectivity index (*SI*) for COX-2 = IC_{50} against COX-1/IC_{50} against COX-2.

On the other hand, the presence of a second aromatic ring in the side chain at C6 of the pyrrolizine scaffold enhanced COX-2 inhibitory activity and selectivity. Compounds **13-15** inhibited activity of COX-2 with IC_{50} values in the range of 0.64-7.53 μM. Among these, compound **14** was the most active and selective as COX-2 inhibitor. Replacement of the (un)substituted phenyl in compounds **13-15** with heteroaryl ring resulted in remarkable decrease in COX-2 inhibitory activity and selectivity. Compounds **16-18** exhibited weaker inhibition in activity of COX-2 compared to compounds **13-15** with pronounce decrease in selectivity, **Table 5**.

Compounds **19-21** displayed inhibitory activity against COX-2 with IC_{50} values in the range of 4.24-52.97 μM. Among these, compound **21** was the most potent as COX-2 inhibitor. Cyclization of the 6-propylideneamino side chain in these compounds into thiazolidinone ring improved COX-2 inhibitory activity and selectivity. On the other hand, the 4-thiazolidinone-bearing indolizine **29** was less active/selective compared to its opened analog **28**, **Table 5**.

2.2.2.2. *In vivo* Anti-inflammatory activity

Based on the results of COXs inhibitory assay, compounds **12**, **14**, **16**, **21** and **24** (the most active COX-2 inhibitors) were selected for evaluation of their *in vivo* anti-inflammatory activity. The reduction in the carrageenan-induced inflammation was used as a measure of their anti-inflammatory activity [47]. Test samples, celecoxib and indomethacin were given orally. The experimental procedures were completed according to our previous report [48]. The results presented in **Table 6**, revealed the ability of the tested compounds to inhibit inflammation with inhibition% in the range of 18.13-44.51%, at 2-4 h after injection of carrageenan.

Table 6. Mean change in edema thickness and anti-inflammatory activity of compounds **12**, **14**, **16**, **21**, **24**, celecoxib and indomethacin.

Compound	Change in edema ± SEM (% inhibition of edema)	
	2h	4h
Control	0.97±0.06 (-)	1.11±0.07 (-)
12	0.79±0.09 (18.13)	0.77±0.11 (30.82)**
14	0.69±0.05 (28.15)	0.62±0.05 (44.51)***
16	0.78±0.13 (18.83)	0.71±0.07 (35.79)**
21	0.78±0.07 (19.17)	0.84±0.08 (24.06)**

24	0.76±0.06 (21.76)	0.75±0.07 (32.48)**
Celecoxib	0.61±0.03 (36.96)*	0.36±0.02 (67.37)***
Indomethacin	0.65±0.03 (32.30)*	0.48±0.04 (56.39)***

Data expressed as mean ± SEM, (n = 6); data were analyzed by One way ANOVA followed by student-Newman-Keuls multiple comparison test, $n = 6$; *P < 0.05 compared to control, **P < 0.01 compared to control, ***P < 0.001 compared to control.

Compound **14** was the most potent as anti-inflammatory agent. It displayed 44.51% inhibition of inflammation (4 h post-carrageenan) compared to 67.37% and 56.39% for celecoxib and indomethacin, respectively. The (hetero)aromatic-bearing derivatives **14** and **16** exhibited higher anti-inflammatory activity as compared with compound **12** (4h post-carrageenan). Moreover, the thiazolidinone-bearing derivative **24** displayed slightly higher anti-inflammatory activity compared to its corresponding Schiff base **21**. However, all of the test compounds were less active than celecoxib and indomethacin. Considering the results of COXs inhibition (**Table 5**), the anti-inflammatory activities of the tested compounds were less than expected. These results can be due to pharmacokinetic issues.

2.2.3. Kinase inhibitory activity

2.2.3.1. Kinases profiling test

Currently, protein kinases are one of the most promising targets in development of new anticancer agents. Based on their rational design, compounds **12**, **19** and **22**, the most active as cytotoxic agents were evaluated for their inhibitory activity against 20 kinases of diverse types and families. The profiling test was performed according to our previous report [21]. Results were summarized in **Table 7**.

Table 7. kinases inhibitory activity of compounds **12**, **19**, **22** and Imatinib.

Kinase	**Compounds**			
	12	**19**	**22**	**Imatinib**
ALK1	**-5%**	**4%**	**-11%**	14%
AMPK (A1/B1/G1)	12%	**-4%**	2%	18%
ASK1	26%	**-14%**	**-3%**	5%
Aurora A	1%	**-8%**	**-11%**	**-38%**
BLK	7%	**-32%**	26%	**-3%**
BRAF	60%	**-15%**	36%	13%
CDK2/cyclin A1	**-4%**	**-34%**	**-23%**	**-2%**
CK1 Alpha 1	6%	**-23%**	**-16%**	0%

DYRK3	**-25%**	33%	38%	**-10%**
EGFR	40%	**-10%**	10%	13%
EPHA1	25%	**-5%**	4%	22%
FLT1	1%	18%	32%	**-10%**
GRK1	1%	**-10%**	**-9%**	2%
GSK3 alpha	**-3%**	**-24%**	**-12%**	**-1%**
MSK1	29%	**-22%**	**-23%**	49%
NEK1	**-14%**	**-1%**	10%	**-2%**
p38 Alpha	33%	2%	5%	17%
PDK1	28%	**-15%**	**-11%**	34%
PRKG1	3%	11%	13%	4%
SGK1	7%	**-14%**	8%	3%

The negative values indicate inhibition in kinase activity, while the positive values indicate the activation of the enzyme.

Compounds **12**, **19** and **20** displayed inhibitory activity for 17 of the selected kinases with inhibition% in the range of 1-34%. The three test compounds displayed the highest inhibitory activity against CDK2/cyclin A1 with inhibition% in the range of 4-34%, compared to only 2% inhibition for imatinib. Moreover, they displayed inhibition of GSK3-α with inhibition% in the range of 3-24%. Moreover, compound **12** reduced activity of NEK1 and , dual specificity tyrosine phosphorylation-regulated kinase 3 (DYRK3) by 14 and 25%, respectively, **Table 7**.

Compound **19** showed inhibitory activity against the largest number of kinases (16 kinases), where the highest inhibitory activity was observed against CDK2 (34%) and B lymphocyte kinase, BLK (32%), **Table 7**.

Moreover, compounds **19** and **22** simultaneously inhibited eight kinases including apoptosis signal-regulating kinase 1 (ASK1), Aurora A, CDK2, CK1 Alpha 1, GRK1, GSK3 alpha, MSK1 and PDK1 with inhibition% in the range of 3-34%. They reduced activity of PDK1 and CK1 Alpha 1 kinases by 11-23%. Compound **19** also exhibited 14% inhibition of the activity of SGK1. The overexpression of PDK1, CK1 Alpha 1 and SGK1 in many types of human tumors [49-51] make them valuable targets in cancer therapy. Accordingly, even small inhibition may contribute partially to the mechanism of action of compounds.

In general, the results in **Table 7** revealed an improvement in kinase inhibitory activity of new compounds as compared to our previously reported pyrrolizine **2** [21]. Compound **2** exhibited inhibitory activity against six kinases (inhibition% = 7-20%), while compounds **12**, **19** and **22** inhibited seventeen kinases (inhibition% = 1-34%).

2.2.3.2. CDK2 inhibitory activity

In kinases profiling test, compounds **12**, **19** and **22** displayed the highest inhibitory activity against CDK2. Accordingly, the three compounds underwent further study to determine their IC_{50} values against CDK2. In this study, kinase inhibitory activity of compounds **12**, **19** and **22** was determined using Adenosine diphosphate (ADP)-Glo kinase assay kit (Promega) according to the previous report [52]. The results revealed potent CDK2 inhibitory activity for the three compounds, **Table 8**. They exhibited IC_{50} values in the (sub)micromolar range against CDK2, compared to imatinib (IC_{50} >100 µM), where compound **19** was the most active (IC_{50} = 0.58 µM).

Table 8. Inhibition of CDK2 by compounds **12**, **19** and **22**.

Comp. No	IC_{50} (µM)[a] ±SEM
12	1.27±0.066
19	0.58±0.029
22	0.63±0.031
Imatinib	>100

[a] Average of three determinations; IC_{50}, concentration which decrease kinase activity to 50%.

2.2.4. Cell cycle analysis

To investigate the mechanism of the new compounds, cell cycle changes in MCF-7 cells treated with the new compounds were analysed. Compounds **12**, **14**, **16** (representing scaffold A) and **22** (representing scaffold B) were selected for this study based on their cytotoxic activity against MCF-7 cells. Flow cytometry was used to analyse propidium iodide (PI)-stained cells according to our previous report [21]. The results of 24 h treatment with the test compounds were outlined in **Table 9**. More than twofold increase in the number of cells in the S-phase was observed after treatment with 1 µM of compounds **12, 14** and **16**. Moreover, this effect was maintained even at higher doses. These results indicated that the three compounds considerably induced cell cycle arrest in the S-phase. On the other hand, compound **22** increased subG1 population, and G1-phase (Figure S114, supplementary data). It was clear from these results that the cell growth arrest caused by compounds **12, 14** and **16** differ from that caused by the thiazolidinone-bearing derivative **22**.

Table 9. Cell cycle analysis of MCF-7 cells treated with compound **12**, **14**, **16** and **22**.

Comp. No	Conc. (μM)	Cell Cycle Stage (%)			
		Sub G1%	G1%	S%	G2/M%
12	0 μM	0.6±0.2	54.6±5.5	17.3±2.5	26.8±4.1
	1μM	1.0±0.1	30.8±5.1	55.6±4.1	12.4±1.4
	5μM	0.9±0.2	30.2±5.3	55.1±3.9	14.4±0.9
	10μM	0.7±0.2	29.6±3.9	55.2±3.4	15.1±2.6
14	0 μM	0.9±0.1	55.1±4.7	18.2±2.2	24.9±3.6
	1μM	0.4±0.1	31.7±6.5	54.1±1.1	14.2±4.5
	5μM	0.4±0.1	28.9±0.4	49.7±3.8	22.0±2.8
	10μM	0.8±0.2	27.9±3.1	51.9±3.3	19.8±1.1
16	0 μM	0.7±0.2	53.9±7.3	17.8±4.1	25.6±2.1
	1μM	1.1±0.4	24.5±0.7	53.7±3.5	22.1±0.9
	5μM	0.4±0.1	25.5±1.9	53.6±2.9	21.8±0.7
	10μM	0.4±0.1	25±0.4	51.5±2.1	23.0±1.6
22	0 μM	3.0±0.8	49.6±2.6	28.5±1.6	17.2±1.5
	1μM	2.4±0.3	56.4±1.6	20.6±1.5	15.6±2.6
	5μM	2.4±0.2	59.4±3.5	17.8±1.6	15.8±1.4
	10μM	8.9±3.2	59.1±1.9	14.2±2.4	14.1±0.3

Data shown in mean % ± SD (n = 2), treatment for 24 h, experiment was repeated 3x.

2.2.5. Apoptosis assay

The programed cell death mechanism (apoptosis) was reported in several cancer cell lines following treatment with COXs inhibitors [53]. Moreover, the anticancer activity of the diarylpyrrolizines **1** and **2** was mediated by induction of apoptosis in colon and breast cancer cells, respectively [20-22]. Accordingly, compounds **12**, **14, 16** and **22** were evaluated for their possible apoptosis inducing activities. Annexin V fluorescein isothiocyanate (FITC)/Propidium Iodide (PI) staining assay was used to determine early and late apoptosis. The assay was performed by treating MCF-7 cells with test compounds according to our previous report [43]. The cells treated with compound **12** (1 μM) showed about twofold increase in apoptotic events (C2: late apoptosis and C4: early apoptosis) compared to control; which increased to more than twofold at 5 and 10 μM. Each of compounds **14** and **16** induced twofold more apoptosis at 1 μM compared to control, while the apoptotic events decreased to onefold at 5 and 10 μM, **Fig. 8**.

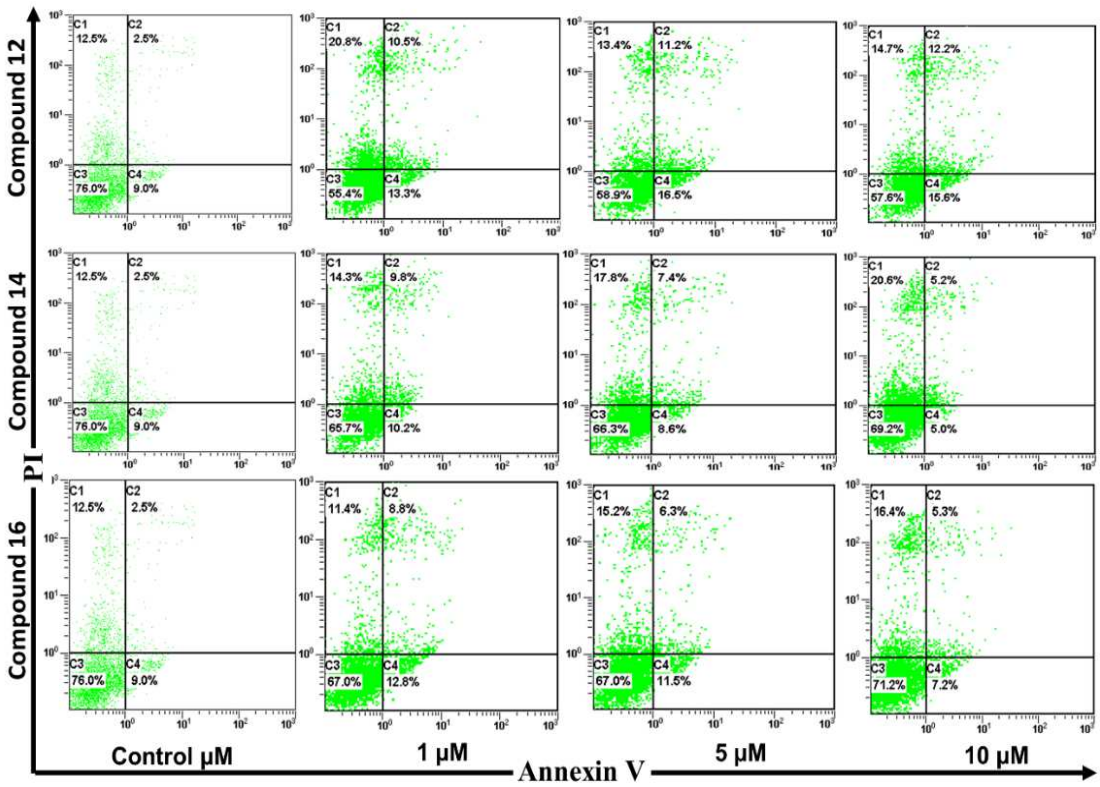

Fig. 8. Annexin V phases of MCF-7 treated with compound **12**, **14** and **16** at 0, 1, 5 and 10 µM (24 h, x axis: Annexin V; y axis: PI). C1: necrotic; C2: late apoptosis; C3: live cells; C4: early apoptosis. Data shown is mean % cell number ± SD (n= 3). Experiment was repeated 3 times.

The results of Annexin V-FITC/PI staining assay for compound **22** (Figure S115, supplementary data). The results revealed significant dose dependent increase in apoptotic events (0%, 19%, 21% and 30% at 0, 1, 5 and 10 µM, respectively). The results were presented

2.3. Molecular docking study

The new compounds displayed weak to strong inhibitory activity against COXs/protein kinases *in vitro*. Docking studies usually provide valuable information about the interactions between ligand and relevant protein which can be used in future optimization of these ligands. In this work, molecular docking studies were performed to explore different types of interaction between the new compounds and COXs/protein kinases. Crystal structure of COXs and protein kinases were obtained from protein data bank (http://www.rcsb.org/pdb/home/home.do). The study was done using AutoDock 4.2 [54]. Visualization of the binding interactions of the new compounds in the active sites of these

proteins was performed by Discovery studio visualizer [55]. The binding free energies and inhibition constants of the new compounds into these enzymes were also evaluated.

2.3.1. Docking study into COX-1 enzyme

In this study, COX-1 crystal structure complexed with ibuprofen (pdb code: 1EQG) [56] was used according to our previous report [57,58]. To validate docking procedures, the native ligand (ibuprofen) was re-docked in COX-1. The results revealed superimposition of the redocked ibuprofen above the co-crystallized ligand with RMSD of 0.87 Å.

The new compounds displayed binding free energy in the range of -7.78 to -9.21 kcal/mol for COX-1, which was higher than licofelone **1** (ΔG_b = -6.83 kcal/mol). Compounds **11-13**, **15-17** and **29** exhibited higher affinity to COX-1 than ibuprofen (ΔG_b = -8.43 kcal/mol for). Moreover, the new compounds displayed inhibition constant in the range of 0.177-1.97 µM compared to 0.664 µM for ibuprofen. Compounds **11** and **28** did not show any conventional hydrogen bonding with the COX-1. However, the remaining compounds displayed up to 5 hydrogen bonds with amino acids in COX-1, compared to three hydrogen bonds for ibuprofen. Like ibuprofen**,** compounds **15** and **16** displayed three hydrogen bonds with the same amino acids (ARG120 and TYR355) in COX-1, **Table 10**.

Among the twelve Schiff bases, compound **16** (ΔG_b = -9.21 kcal/mol) displayed the highest binding free energy to COX-1, while compound **29** (ΔG_b = -8.74 kcal/mol) showed the best affinity for COX-1 among the four thiazolidinone-bearing derivatives **22-24** and **29**. Compounds **22** and **29** displayed slightly higher binding affinity for COX-1 than their corresponding analogs **19** and **28**, **Table 10**.

Table 10. Results of the docking study of compounds **11-24, 28, 29,** licofelone **1** and ibuprofen into COX-1 (pdb: 1EQG) [56].

Ligand	ΔG_b [a]	K_i [b]	HBs [c]	Atoms in H-bonding		Length [d] (Å)
				In ligand	Amino acid	
11	-8.62	0.484 µM	- [e]	-	-	-
12	-8.94	0.278 µM	1	7-CN	OH of SER530	2.55
13	-8.67	0.438 µM	2	CONH	NH of ARG120	2.28
				CONH	OH of TYR355	2.57
14	-8.33	0.777 µM	2	CONH	NH_2 of ARG120	2.28
				CONH	OH of TYR385	2.32
15	-9.11	0.211 µM	3	CONH	NH_2 of ARG120	2.21
				CONH	OH of TYR355	2.43

				CONH	NH of ARG120	3.03
16	-9.21	0.177 µM	3	Furanyl O	NH_2 of ARG120	1.68
				Furanyl O	OH of TYR355	2.13
				N=CH	OH of TYR355	2.90
17	-8.74	0.389 µM	2	CONH	OH of TYR385	2.13
				CONH	NH_2 of ARG120	2.39
18	-7.94	1.520 µM	2	CONH	NH_2 of ARG120	2.12
				CONH	OH of TYR355	2.29
19	-7.78	1.970 µM	5	CN	NH_2 of ARG83	2.73
				CN	NH of ARG83	2.63
				N=CH	NH_2 of ARG120	2.33
				CONH	NH_2 of ARG120	1.83
				CONH	OH of TYR355	2.23
20	-8.33	0.782 µM	1	CN	OH of SER530	2.53
21	-8.26	0.879 µM	5	CN	NH of ARG83	2.85
				CN	NH_2 of ARG83	2.94
				N=CH	NH_2 of ARG120	2.37
				CONH	NH_2 of ARG120	1.92
				CONH	OH of TYR355	1.95
22	-8.04	1.270 µM	2	CN	NH_2 of ARG83	2.06
				CN	NH of ARG83	2.94
23	-8.11	1.140 µM	2	CN	NH_2 of ARG83	1.84
				CN	NH of ARG83	2.62
24	-8.14	1.070 µM	2	PhNHCO	NH_2 of ARG83	2.09
				PhNHCO	OH of TYR355	2.12
				S	NH of ARG83	2.96
28	-8.26	0.877 µM	-[e]	-	-	-
29	-8.74	0.389 µM	2	PhNHCO	NH_2 of ARG83	1.89
				PhNH	CO of GLU524	2.29
1	-6.83	9.870 µM	1	COOH	NH_2 of ARG83	2.49
Ibu.	-8.43	0.664 µM	3	C=O	NH of ARG120	1.71
				COOH	NH_2 of ARG120	1.79
				COOH	OH of TYR355	1.83

[a] Binding free energy (kcal/mol); [b] Inhibition constant (µM); [c]HBs, number of hydrogen bonds; [d] length in angstrom (Å); [e] No hydrogen bond detected

2.3.2. Docking study into COX-2 enzyme

The binding modes of the new compounds into COX-2 (pdb code: 1CX2) [59] were evaluated in a docking study using AutoDock 4.2, according to the previous report [57,58]. SC-558 was initially re-docked into the active site of COX-2 to validate docking procedures. The result revealed superimposition of the redocked ligand above native SC-558 with RMSD of 1.56 Å. The new compounds displayed high binding affinity to COX-2 (ΔG_b = -8.92 to -11.86 kcal/mol), **Table 11**.

Table 11. Docking results of compounds **11-24**, **28**, **29**, licofelone **1** and SC-588 into COX-2 (pdb: 1CX2) [59].

Ligand	ΔG_b [a]	K_i [b]	HBs [c]	Atoms in H-bonding		Length [d] (Å)
				In ligand	In protein	
11	-9.45	119.07 nM	1	CONH	OH of TYR355	1.81
12	-10.17	35.34 nM	2	CONH	OH of TYR355	1.76
				CONH	NH_2 of ARG120	3.38
13	-11.86	2.03 nM	- [e]	-	-	-
14	-11.47	3.94 nM	2	7-CN	OH of SER530	3.55
				CONH	NH_2 of ARG513	3.82
15	-10.93	9.7 nM	2	7-CN	OH of SER530	3.49
				CONH	NH_2 of ARG120	2.95
16	-10.63	16.12 nM	2	Furanyl O	NH of ALA527	3.23
				CONH	NH_2 of ARG513	3.79
17	-11.23	5.88 nM	2	7-CN	OH of SER530	3.41
				CONH	NH_2 of ARG513	3.91
18	-11.33	4.96 nM	3	7-CN	OH of SER530	3.52
				Pyridinyl N	NH of GLY526	3.61
				CONH	NH_2 of ARG513	3.84
19	-9.2	179.06 nM	2	CONH	CO of VAL523	1.93
				6-N=CH	OH of TYR355	2.59
20	-8.92	289.37 nM	- [e]	-	-	-
21	-9.14	198.07 nM	- [e]	-	-	-
22	-9.74	72.18 nM	1	CONH	CO of LEU352	2.53
23	-9.92	53.54 nM	1	CN	OH of SER530	2.65
24	-10.05	43.29 nM	1	CN	OH of SER530	2.72
28	-9.13	203.67 nM	1	Ph CONH	CO of LEU352	2.16
29	-10.14	36.98 nM	3	Ph CONH	CO of VAL523	2.11
				CN	NH of ARG120	2.06
				CN	OH of TYR355	2.57
1	-8.75	383.87 nM	- [e]	-	-	-
SC-588	-10.74	13.38 nM	4	O of SO_2	NH of HIS90	2.03
				H^1 of NH_2	CO of LEU352	2.11
				H^2 of NH_2	CO of GLN192	2.09
				CF_3	NH of ARG120	2.46

[a] Binding free energy (kcal/mol); [b] Inhibition constant (nM); [c] HBs, number of hydrogen bonds; [d] length in angstrom (Å); [e] No hydrogen bond detected.

Moreover, these compounds exhibited inhibition constant in the range of 2.03-289.37 nM against COX-2 compared to 13.38 nM for SC-558, **Table 11**. Compound **13** displayed the highest binding affinity to COX-2, while compound **20** showed the lowest affinity. Compounds **13**, **20** and **21** did not show any conventional hydrogen bonds with COX-2 although the remaining compounds displayed 1-3 hydrogen bonds.

Compounds **13-18** with the (hetero)aromatic rings in the side chain at C6 displayed higher binding affinity than those bearing aliphatic side chain (**11** and **12**). In addition, the 4-

thiazolidinone-bearing derivatives **22**-**24** and **29** showed also higher affinity for COX-2 than their corresponding Schiff bases **19**-**21** and **28**, **Table 11**.

To visualize different types of bonding interactions between the new compounds and COX-1/2, compounds **13** and **24** were selected based on their high affinities to COX-2. Compound **13** exhibited inhibition constants (K_i) of 438 and 2.03 nM for COX-1 and COX-2, respectively, indicating high selectivity for COX-2, **Table 10** and **11**. These results were in accordance with the results of COXs inhibition assay, **Table 5**.

Several interactions of hydrophilic and hydrophobic types were observed between compound **13** and COX-1. Among these interactions, two conventional hydrogen bonds were detected with ARG120 and TYR355. In addition, compound **13** formed up to fourteen hydrophobic interactions with the hydrophobic residues in the active site of COX-1, **Fig. 9**. No conventional hydrogen bonds were observed between compound **13** and COX-2. Instead, other types of interactions including carbon hydrogen bond, halogen, pi-cation, pi-sulfur and amide-pi stacked interactions were observed. Compound **13** displayed also pi-sigma, alkyl and pi-alkyl hydrophobic interactions with the hydrophobic residues in COX-2, (Figure S116, supplementary data).

Moreover, compound **24** displayed inhibition constants of 1070 and 43.29 nM for COX-1 and COX-2, respectively, indicating high potential selectivity for COX-2. These findings are matched with the results of *in vitro* COXs inhibition assay, where compound **24** showed SI >86 for COX-2, **Table 5**. Investigation of the binding mode of compound **24** revealed two conventional hydrogen bonds with COX-1 and only one conventional hydrogen bond with COX-2, **Fig. 9**. The higher affinity to COX-2 could be attributed to the presence of pi-cation interaction with ARG513, and two pi-sulfur interactions with TYR385 and TRP387 amino acids, (Figure S117, supplementary data).

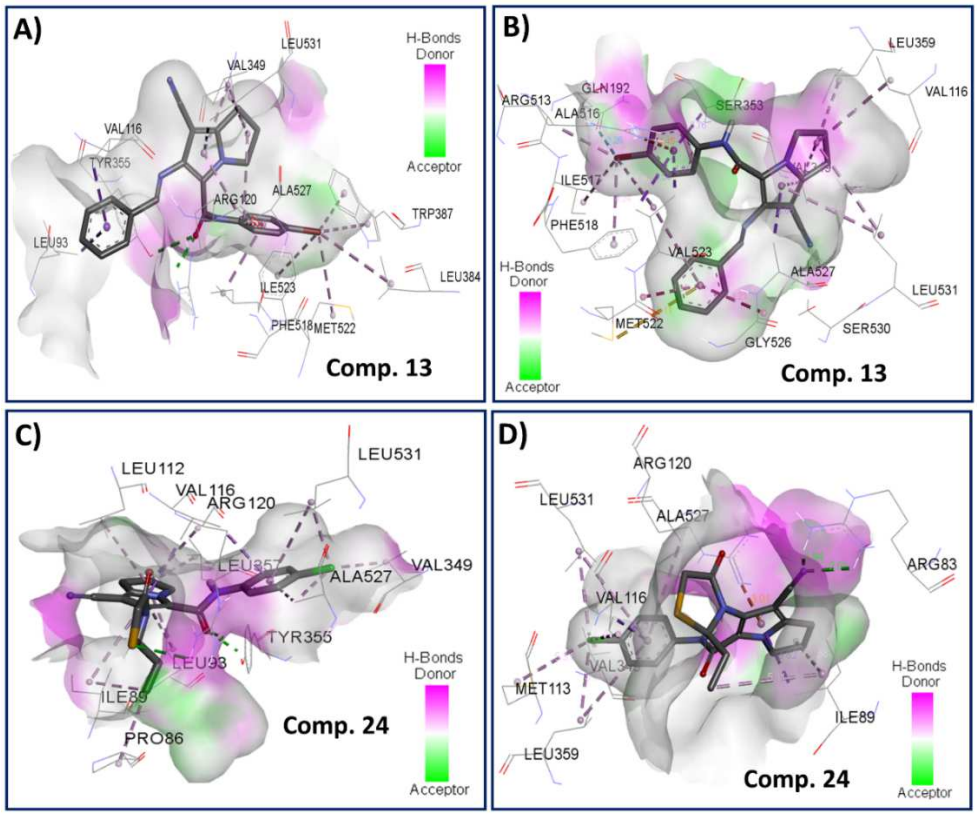

Fig. 9. Binding modes/interactions of compound **13** and **24 (**shown as stick, colored by element) into the active site of COXs: A) 3D binding mode of compound **13** into COX-1 ; B) 3D binding mode of compound **13** into COX-2; C) 3D binding mode of compound **24** into COX-1 ; D) 3D binding mode of compound **24** into COX-2; hydrogen bonds represented by green dotted line; receptor surface shown as H-bond donor (red)/acceptor (green); hydrogen atoms were omitted for clarity.

Interestingly, the propylideneamino-bearing derivatives (**11**, **19-21** and **28**) displayed high binding affinities to COX-1/2, although no hydrogen bonding interaction was observed. That was due to formation of other types of interaction such as carbon-hydrogen and hydrophobic interactions. Among these derivatives, compound **11** exhibited two carbon hydrogen bonds with COX-1, while compound **28** showed only one bond. The two compounds displayed different types of hydrophobic interactions including pi-sigma, alkyl and pi-alkyl types, (Figure S118, supplementary data).

Similarly, compounds **20** and **21** showed good affinity to COX-2 without forming any conventional hydrogen bonds with this enzyme. Compound **20** displayed two carbon hydrogen bonds with VAL523 and SER530, while compound **21** formed only one carbon hydrogen bond with VAL523. The two compounds also displayed different types of hydrophobic interactions, (Figure S118, supplementary data).

In general, all the new compounds displayed higher affinity for COX-2 than COX-1. These results are matched with the results of the *in vitro* COX inhibition assay. The conventional hydrogen bonds formed between the new compounds and COX-1/2 enzymes contributed to their overall binding affinity. However, the hydrogen bonds formed with COX-2 are longer and weaker than those formed with COX-1, **Tables 10** and **11**. These results indicated that the new compounds interact mainly by hydrophobic interactions with COX-1/2. These interactions contribute significantly to the overall bonding affinity of these compounds.

2.3.3. Docking study into protein kinases

Targeting oncogenic protein kinases with inhibitors has proven success in treatment of different types of cancers [60]. Understanding the nature of the interactions between these inhibitors provided a useful tool in the design new of potent kinase inhibitors [43]. In this work, a comparative docking study of compounds **12**, **19** and **22** into PKs was performed by AutoDock 4.2. Four kinases including CDK2, Aurora A, BRAF, and EGFR were selected for this study based on the results of kinase inhibition assay, **Tables 7** and **8**. The crystal structure of CDK2 (pdb code: 3TNW) [61], Aurora A (pdb code: 3E5A) [62], BRAF (pdb code: 4RZV) [63] and EGFR (pdb code: 1M17) [64] were obtained from protein data bank. The native ligands were redocked into the active sites of their corresponding PKs to validate docking procedures. The results of the study were summarized in **Table 12**.

Table 12. Docking results of compounds **12, 19, 22** into CDK2, Aurora A, BRAF and EGFR kinases in comparison to their native ligands.

PK (pdb)	**Ligand**	ΔG_b [a]	K_i [b]	**PK** (pdb)	**Ligand**	ΔG_b [a]	K_i [b]
CDK2	**12**	-8.04	1.290 µM	**BRAF**	**12**	-9.29	154.4 nM
(3TNW)	**19**	-7.63	2.550 µM	(4RZV)	**19**	-8.69	424.84 nM
	22	-8.35	0.754 µM		**22**	-9.18	186.6 nM
	CAN508 [c]	-6.47	18.20 µM		**Vemurafenib**	-12.77	432.93 nM
Aurora A	**12**	-8.81	346.04 nM	**EGFR**	**12**	-8.51	577.35 nM
(3E5A)	**19**	-7.48	3.27 µM	(1M17)	**19**	-7.31	4.37 µM
	22	-8.32	801.79 nM		**22**	-8.12	1.12 µM
	VX6 [d]	-8.49	602.62 nM		**Erlotinib**	-7.39	3.84 µM

[a] Binding free energy (kcal/mol).

[b] Inhibition constant.

[c] CAN508, (*E*)-4-((3,5-diamino-1*H*-pyrazol-4-yl)diazenyl)phenol.

[d] VX6, *N*-(4-((4-((3-methyl-1*H*-pyrazol-5-yl)amino)-6-(4-methylpiperazin-1-yl)pyrimidin-2-yl)thio)phenyl)cyclopropanecarboxamide.

The re-docked CDK2-ligand (CAN508) superimposed over native ligand with RMSD of 1.11 Å. Compounds **12**, **19** and **22** displayed higher affinities (ΔG_b = -7.63 to -8.35 kcal/mol) for CDK2 than CAN508 (ΔG_b = -6.47 kcal/mol). The affinity of compound **22** to CDK2 was higher than that of compound **12**, which was matched with their results in kinase profiling test, **Tables 7**. The 3D binding modes of compounds **12**, **19** and **22** into CDK2 were generated by performed with Discovery Studio Visualizer, (Figure S119, supplementary data).

A 2D plot (**Fig. 10**) showing the binding interactions of compound **19** with CDK2 was generated by LigPlot^{+} (v.2.1) [65]. Both hydrophobic and hydrogen bonding interactions of compound **19** were presented in this figure in comparison with that of the re-docked ligand (CAN508). Compound **19** displayed two hydrogen bonds with ILE10 and LYS89 compared to four hydrogen bonds for CAN508. However, compound **19** displayed higher affinity to CDK2 than CAN508 which was due to the larger number of hydrophobic interactions formed.

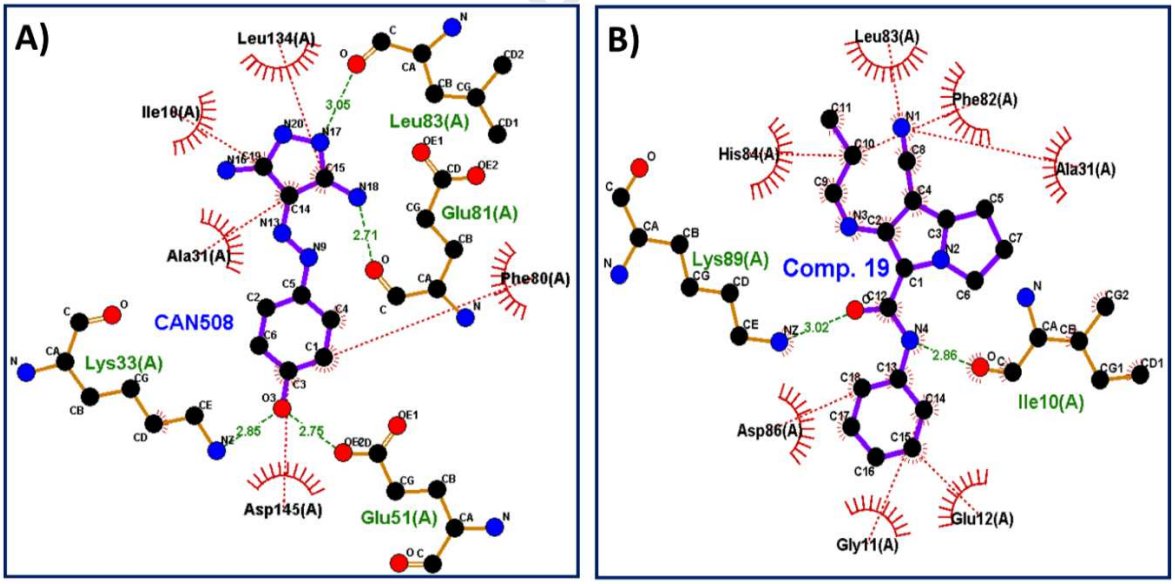

Fig. 10. A) LigPlot view of CAN508 redocked into the active site of CDK2 (pdb: 3TNW); B) LigPlot view of compound **19** into CDK2; ligand bonds shown in purple, hydrophobic interactions shown in brick red dotted lines and hydrogen bonding interactions shown in olive green dotted lines.

3. Conclusions

Two new series of pyrrolizine-5-carboxamides were synthesized and evaluated for their cytotoxicity and anti-inflammatory activities. The new compounds exhibited potent cytotoxicity (IC_{50} = 0.10-22.96 μM) against three cancer (MCF-7, A2780 and HT29) cell lines with selectivity index in the range of 1-258 toward cancer cells. Among these derivatives, compound **12** displayed the highest cytotoxicity against MCF-7 cells, while compound **23** was the most active against both A2780 and HT29 cell lines. Moreover, the new compounds also exhibited significant anti-inflammatory activity (18.13-44.51% inhibition of inflammation) mediated by inhibition of COX-1/2 with preferential inhibition of COX-2. The study of SAR revealed favorable cytotoxic outcomes of the aliphatic side chain and 4-thiazolidinone moiety at C6 of the pyrrolizine nucleus, while aromatic side chain enhanced anti-inflammatory activities. The results of kinase profiling of compounds **12**, **19** and **22** revealed weak to moderate inhibition of multiple kinases. Moreover, the three compounds inhibited the activity of CDK2 with IC_{50} values in the (sub)micromolar range against, where compound **19** was the most active (IC_{50} = 0.58 μM). Cell cycle analysis of MCF-7 cells treated with compounds **12**, **14** and **16** revealed more than twofold increase in cells in the S-phase, while compound **22** increased number of cells in subG1 population and G1-phase. Moreover, compounds **12**, **14** and **16** induced about twofold increase in apoptotic events in MCF-7 cells at 1 μM, while compound **22** increased apoptotic events by 19%. Docking study of the new compounds revealed nice fitting into COX-1/2 with higher affinity toward COX-2. Moreover, compounds **12**, **19** and **22** exhibited also higher affinities for CDK2 compared to CAN508. To sum up, the above-mentioned data highlight these compounds as promising anticancer and anti-inflammatory agents.

4. Experimental

4.1. Chemistry

The infrared (IR) spectra of the new compounds were recorded using BRUKER TENSOR 37 FTIR spectrophotometer. The spectra were measured using KBr disc and expressed as wave number (cm^{-1}). Shimadzu Qp-2010 Plus mass spectrometer with EI ionization mode was used to record the mass spectra of the new compounds. The quantitative elemental analyses (C,H, and N) were measured in Microanalytical Center, Cairo University. ^{1}H-NMR, ^{13}C-NMR and DEPT C^{135} spectra were recorded in the specified solvent using BRUKER AVANCE III at 500 MHz, 125 and 125 MHz, respectively. Spectra data including IR, mass, ^{1}H-NMR, ^{13}C-NMR and DEPT C^{135} spectra of the new compounds were provided in supplementary data.

Preparation of the starting compounds **7**, **9a-d**, **10a-d**, **26** and **27** was performed using the synthetic procedures of the previous reports [38-41]. Purity of the starting and new compounds was checked using TLC. After purification, melting points (uncorrected) were determined by digital melting point apparatus (IA 9100MK series). Solvents and chemical reagents were purchased from Sigma-Aldrich.

4.1.1. General procedure (A) for the preparation of compounds (11-21 and 28).

The Schiff bases (**11-21** and **28**) were prepared from the reaction of the appropriate aldehyde (2.4-10 mmol) with the appropriate stating compound (**10a-d** and **27**, 2 mmol) in absolute ethanol (40 mL). Glacial acetic acid (0.5 mL) was added to reaction mixture. The reaction mixture was stirred at 40-50 °C for 2 h followed by refluxing for 6h. After cooling, the solvent was evaporated under reduced pressure. The formed precipitate was recrystallized from chloroform-acetone (1:1). The yield% and melting points of the new compounds were summarized in **Table 1**.

4.1.1.1. (*E*)-*N*-(4-Bromophenyl)-7-cyano-6-(propylideneamino)-2,3-dihydro-1*H*-pyrrolizine-5-carboxamide (11)

The title compound was prepared from the reaction of compound **10a** (0.69 g, 2 mmol) with propionaldehyde (0.58 g, 10 mmol) according to the general procedure A. Compound **11** was obtained as white solid product. IRυ_{max}/cm^{-1} 3219 (NH), 3099 (Ar C-H), 2917 (Aliphatic C-H), 2214 (CN), 1664 (C=O), 1638, 1550 (C=C, C=N), 1478, 1392, 1289 (C-C, C-N), 506 (C-Br). ^{1}H-NMR ($CDCl_3$, 500 MHz, δ ppm): 1.35 (t, 3H, J = 7.3 Hz, -$CH_2C\underline{H}_3$), 2.54-2.60 (m, 2H, pyrrolizine CH_2-2), 2.65-2.70 (m, 2H, -$C\underline{H}_2CH_3$), 3.05 (t, 2H, J = 7.5 Hz, CH_2-1),

4.52 (t, 2H, *J* = 7.2 Hz, CH_2-3), 7.46 (d, 2H, *J* = 8.7 Hz, phenyl CH-3 + CH-5), 7.55 (d, 2H, *J* = 8.7 Hz, phenyl CH-2 + CH-6), 8.76 (t, *J* = 3.7, H, N=CH), 10.70 (s, H, CONH). ^{13}C-NMR ($CDCl_3$, 125 MHz, δ ppm): 9.62 ($\underline{C}H_3CH_2$), 24.54 (pyrrolizine $\underline{C}H_2$-2), 25.45 ($CH_3\underline{C}H_2$), 30.11 (pyrrolizine $\underline{C}H_2$-1), 50.01 (pyrrolizine $\underline{C}H_2$-3), 96.27 (pyrrolizine $\underline{C}$-7), 103.12 ($\underline{C}N$), 116.22 ($\underline{C}$-6), 121.17 (phenyl $\underline{C}$H-2 + $\underline{C}$H-6), 125.74 (pyrrolizine $\underline{C}$-5), 131.99 (phenyl $\underline{C}$H-3 + $\underline{C}$H-5), 133.93 (phenyl C-4), 137.85 ($\underline{C}$-7a), 139.38 (phenyl $\underline{C}$-1), 164.78 (N=$\underline{C}$H), 167.93 ($\underline{C}$ONH). DEPT C^{135} ($CDCl_3$, 125 MHz, δ ppm): 9.63 ($\underline{C}H_3CH_2$), 24.55 (pyrrolizine $\underline{C}H_2$-2), 25.45 ($CH_3\underline{C}H_2$), 30.12 (pyrrolizine $\underline{C}H_2$-1), 50.01 (pyrrolizine $\underline{C}H_2$-3), 121.17 (phenyl $\underline{C}$H-2 + $\underline{C}$H-6), 131.99 (phenyl $\underline{C}$H-3 + $\underline{C}$H-5). MS (EI): m/z (%) 384 (M^+, 2), 358 (26), 357 (100), 356 (20), 355 (92), 276 (6), 198 (3), 171 (4), 152 (34), 130 (4), 123 (6), 104 (5), 92 (4), 77 (5). Anal. Calcd. for $C_{18}H_{17}BrN_4O$ (385.26): C, 56.12; H, 4.45; N, 14.54; Found: C, 55.81; H, 4.73; N, 14.67.

4.1.1.2. (*E*)-*N*-(4-Bromophenyl)-7-cyano-6-((3-methylbutylidene)amino)-2,3-dihydro-1*H*-pyrrolizine-5-carboxamide (12)

The title compound was prepared from the reaction of compound **10a** (0.69 g, 2 mmol) with isovaleraldehyde (0.21 g, 2.4 mmol) according to the general procedure A. Compound **12** was obtained as white solid product. IRυ_{max}/cm^{-1} 3343 (NH), 3067 (Ar C-H), 2958 (Aliphatic C-H), 2213 (CN), 1671 (C=O), 1638, 1592 (C=C, C=N), 1457, 1315, 1246 (C-C, C-N), 507 (C-Br). ^{1}H-NMR ($CDCl_3$, 500 MHz, δ ppm): 1.10 (d, 6H, *J* = 6.5 Hz, CH($C\underline{H}_3$)$_2$), 2.14-2.22 (m, H, C$\underline{H}$(CH$_3$)$_2$), 2.50 (t, 2H, *J* = 5.7 Hz, N=CH-C$\underline{H}_2$), 2.54-2.60 (m, 2H, pyrrolizine CH_2-2), 3.04 (t, 2H, *J* = 7.5 Hz, pyrrolizine CH_2-1), 4.51 (t, 2H, *J* = 7.2 Hz, pyrrolizine CH_2-3), 7.47 (d, 2H, *J* = 8.1 Hz, phenyl CH-3 + CH-5), 7.53 (d, 2H, *J* = 8.2 Hz, phenyl CH-2 + CH-6), 8.74 (t, H, *J* = 4.8 Hz, N=CH), 10.66 (s, H, CONH). ^{13}C-NMR ($CDCl_3$, 125 MHz, δ ppm): 22.65 (CH($\underline{C}H_3$)$_2$), 24.52 (pyrrolizine $\underline{C}H_2$-2), 25.45 (pyrrolizine $\underline{C}H_2$-1), 26.40 ($\underline{C}$H(CH$_3$)$_2$), 46.06 (N=CH-$\underline{C}H_2$), 49.96 (pyrrolizine $\underline{C}H_2$-3), 115.95 (pyrrolizine $\underline{C}$-7), 116.16 ($\underline{C}$N), 116.69 (pyrrolizine $\underline{C}$-6), 121.02 (phenyl $\underline{C}$H-2 + $\underline{C}$H-6), 128.72 (phenyl $\underline{C}$-4), 131.97 (phenyl $\underline{C}$H-3 + $\underline{C}$H-5), 137.57 (pyrrolizine C-5), 139.54 (pyrrolizine $\underline{C}$-7a), 147.81 (phenyl $\underline{C}$-1), 158.46 (N=$\underline{C}$H), 167.28 ($\underline{C}$ONH). DEPT C^{135} ($CDCl_3$, 125 MHz, δ ppm): 22.65 (CH($\underline{C}H_3$)$_2$), 24.53(pyrrolizine $\underline{C}H_2$-2), 25.45 (pyrrolizine $\underline{C}H_2$-1), 26.40 ($\underline{C}$H(CH$_3$)$_2$), 46.06 (N=CH-$\underline{C}H_2$), 49.96 (pyrrolizine $\underline{C}H_2$-3), 121.02 (phenyl $\underline{C}$H-2 + $\underline{C}$H-6), 132.02 (phenyl $\underline{C}$H-3 + $\underline{C}$H-5). MS (EI): m/z (%) 412 (M^+, 2), 358 (16), 357 (82), 356 (20), 355 (100), 242 (11), 200 (12), 186 (8), 172 (6), 158 (4), 145 (6), 130

(4), 104 (2), 91 (4), 77 (2). Anal. Calcd. for $C_{20}H_{21}BrN_4O$ (413.31): C, 58.12; H, 5.12; N, 13.56; Found: C, 57.81; H, 4.76; N, 13.67.

4.1.1.3. (*E*)-6-(Benzylideneamino)-*N*-(4-bromophenyl)-7-cyano-2,3-dihydro-1*H*-pyrrolizine-5-carboxamide (13)

The title compound was prepared from the reaction of compound **10a** (0.69 g, 2 mmol) with benzaldehyde (0.25 g, 2.4 mmol) according to the general procedure A. Compound **13** was obtained as yellow solid product. IRυ_{max}/cm^{-1} 3385 (NH), 3001 (Ar C-H), 2912 (Aliphatic C-H), 2206 (CN), 1669 (C=O), 1596, 1543 (C=C, C=N), 1428, 1391, 1309 (C-C, C-N), 520 (C-Br). ^{1}H-NMR ($CDCl_3$-500 MHz) δ (ppm): 2.58-2.62 (m, 2H, pyrrolizine CH_2-2), 3.09 (t, 2H, J = 7.5 Hz, pyrrolizine CH_2-1), 4.57 (t, 2H, J = 7.5 Hz, pyrrolizine CH_2-3), 7.48-7.58 (m, 7H, aromatic Hs), 7.95 (d, 2H, J = 5.7, CH-2 + CH-6), 9.22 (s, H, N=CH), 10.75 (s, H, CONH). ^{13}C-NMR ($CDCl_3$, 125 MHz, δ ppm): 24.58 (pyrrolizine $\underline{C}H_2$-2), 25.44 (pyrrolizine $\underline{C}H_2$-1), 50.14 (pyrrolizine $\underline{C}H_2$-3), 116.36 (pyrrolizine $\underline{C}$-7), 121.11 (phenyl $\underline{C}$H-2′ + $\underline{C}$H-6′), 128.72 (phenyl CH-3″ + CH-5″), 129.02 ($\underline{C}$N), 129.22 (phenyl CH-2″ + CH-6″), 129.77 (pyrrolizine $\underline{C}$-6), 130.46 (phenyl C4′), 132.06 (phenyl CH-3′ + CH-5′), 132.60 (phenyl CH-4″), 135.32 (pyrrolizine C5), 137.43 (pyrrolizine C-7a), 139.33 (phenyl C-1″), 148.42 (phenyl C-1′), 158.46 (N=$\underline{C}$H), 160.02 ($\underline{C}$ONH). DEPT C^{135} ($CDCl_3$, 125 MHz, δ ppm): 24.58 (pyrrolizine $\underline{C}H_2$-2), 25.44 (pyrrolizine $\underline{C}H_2$-1), 50.14 (pyrrolizine $\underline{C}H_2$-3), 121.11 (phenyl $\underline{C}$H-2′ + $\underline{C}$H-6′), 128.72 (phenyl CH-3″ + CH-5″), 129.22 (phenyl CH-2″ + CH-6″), 132.06 (phenyl CH-3′ + CH-5′), 132.60 (phenyl CH-4″). MS (EI): m/z (%) 434 (M^++2, 5), 433 (M^++1, 2), 432 (M^+, 5), 357 (8), 263 (18), 262 (100), 234 (6), 206 (4), 176 (4), 105 (2), 91 (2), 77 (4). Anal. Calcd. for $C_{22}H_{17}BrN_4O$ (433.30): C, 60.98; H, 3.95; N, 12.93; Found: C, 61.45; H, 4.13; N, 13.47.

4.1.1.4. (*E*)-*N*-(4-Bromophenyl)-7-cyano-6-((4-hydroxybenzylidene)amino)-2,3-dihydro-1*H*-pyrrolizine-5-carboxamide (14)

The title compound was prepared from the reaction of compound **10a** (0.69 g, 2 mmol) with 4-hydroxybenzaldehyde (0.29 g, 2.4 mmol) according to the general procedure A. Compound **14** was obtained as yellow solid product. IRυ_{max}/cm^{-1} 3324 (NH), 3060 (Ar C-H), 2898 (Aliphatic C-H), 2211 (CN), 1669 (C=O), 1598, 1579 (C=C, C=N), 1475, 1392, 1278 (C-C, C-N, C-O), 509 (C-Br). ^{1}H-NMR (DMSO-500 MHz) δ (ppm): 2.43-2.51 (m, 2H, pyrrolizine CH_2-2), 2.97 (t, 2H, J = 7.4 Hz, pyrrolizine CH_2-1), 4.34 (t, 2H, J = 7.1 Hz, pyrrolizine CH_2-3), 5.55 (s, H, OH), 6.97 (d, 2H, J = 8.4, phenyl CH-3′+ CH-5′), 7.53 (d,

2H, *J* = 8.7, phenyl CH-3″+ CH-5″), 7.57 (d, 2H, *J* = 8.8, phenyl CH-2′ + CH-6′), 7.82 (d, 2H, *J* = 8.3, phenyl CH-2″+ CH-6″), 8.88 (s, H, N=CH), 10.49 (s, H, CONH). ^{13}C-NMR (DMSO, 125 MHz, *δ* ppm): 24.50 (pyrrolizine $\underline{C}H_2$-2), 25.40 (pyrrolizine $\underline{C}H_2$-1), 50.32 (pyrrolizine $\underline{C}H_2$-3), 76.60 (pyrrolizine $\underline{C}$-7), 115.48 ($\underline{C}N$), 115.99 (pyrrolizine C-6), 116.36 (phenyl C-4′), 116.87 (phenyl $\underline{C}H$-3″ + $\underline{C}H$-5″), 121.30 (phenyl $\underline{C}H$-2′ + $\underline{C}H$-6′), 126.43 (phenyl C-1″), 131.49 (phenyl $\underline{C}H$-2″ + $\underline{C}H$-6″), 132.36 (phenyl $\underline{C}H$-3′ + $\underline{C}H$-5′), 138.07 (pyrrolizine C-5), 140.97 (pyrrolizine C-7a), 149.16 (phenyl $\underline{C}$-1′), 158.23 (phenyl C-4″), 160.86 (N=$\underline{C}H$), 162.74 ($\underline{C}$ONH). DEPT C^{135} (DMSO, 125 MHz, *δ* ppm): 24.50 (pyrrolizine $\underline{C}H_2$-2), 25.40 (pyrrolizine $\underline{C}H_2$-1), 50.32 (pyrrolizine $\underline{C}H_2$-3), 116.87 (phenyl CH-3″ + CH-5″), 121.30 (phenyl $\underline{C}H$-2′ + $\underline{C}H$-6′), 131.49 (phenyl CH-2″ + CH-6″), 132.36 (phenyl CH-3′ + CH-5′). MS (EI): m/z (%) 450 (M^++2, 2), 449 (M^++1, 1), 448 (M^+, 2), 357 (2), 330 (7), 279 (19), 278 (100), 250 (14), 234 (7), 222 (18), 195 (14), 184 (21), 174 (28), 156 (9), 146 (9), 132 (5), 121 (9), 104 (4), 91 (11), 77 (13). Anal. Calcd. for $C_{22}H_{17}BrN_4O_2$ (449.30): 58.81; H, 3.81; N, 12.47; Found: C, 59.12; H, 4.22; N, 12.27.

4.1.1.5. (*E*)-*N*-(4-Bromophenyl)-6-((4-chlorobenzylidene)amino)-7-cyano-2,3-dihydro-1*H*-pyrrolizine-5-carboxamide (15)

The title compound was prepared from the reaction of compound **10a** (0.69 g, 2 mmol) with 4-chlorobenzaldehyde (0.34 g, 2.4 mmol) according to the general procedure A. Compound **15** was obtained as yellow solid product. IRυ_{max}/cm^{-1} 3343 (NH), 3002 (Ar C-H), 2894 (Aliphatic C-H), 2214 (CN), 1671 (C=O), 1595, 1546 (C=C, C=N), 1474, 1417, 1393 (C-C, C-N), 520 (C-Br). ^{1}H-NMR ($CDCl_3$-500 MHz) *δ* (ppm): 2.58-2.64 (m, 2H, pyrrolizine CH_2-2), 3.09 (t, 2H, *J* = 7.6 Hz, pyrrolizine CH_2-1), 4.56 (t, 2H, *J* = 7.3 Hz, pyrrolizine CH_2-3), 7.50 (d, 2H, *J* = 8.1, phenyl CH-3″ + CH-5″), 7.56 (d, 4H, *J* = 6.0, Ar CH-3′+CH-5′+CH-2′+CH-6′), 7.88 (d, 2H, *J* = phenyl 8.3, CH-2″ + CH-6″), 9.18 (s, H, N=CH), 10.61 (s, H, CONH). ^{13}C-NMR ($CDCl_3$, 125 MHz, *δ* ppm): 24.59 (pyrrolizine $\underline{C}H_2$-2), 25.47 (pyrrolizine $\underline{C}H_2$-1), 50.15 (pyrrolizine $\underline{C}H_2$-3), 115.17 (pyrrolizine $\underline{C}$-7), 116.09 ($\underline{C}N$), 116.39 (pyrrolizine $\underline{C}$-6), 117.69 (phenyl $\underline{C}H$-4′), 121.15 (phenyl $\underline{C}H$-2′ + $\underline{C}H$-6′), 128.71 (phenyl $\underline{C}H$-3″ + $\underline{C}H$-5″), 129.22 (phenyl $\underline{C}H$-2″ + $\underline{C}H$-6″), 132.08 (phenyl $\underline{C}H$-3′ + $\underline{C}H$-5′), 132.57 (pyrrolizine $\underline{C}$-5), 135.39 (phenyl $\underline{C}H$-1″), 137.44 (pyrrolizine $\underline{C}H$-7a), 139.43 (phenyl $\underline{C}H$-4″), 148.38 (phenyl $\underline{C}H$-1′), 158.50 (N=$\underline{C}H$), 160.05 ($\underline{C}$ONH). DEPT C^{135} ($CDCl_3$, 125 MHz, *δ* ppm): 24.60 (pyrrolizine $\underline{C}H_2$-2), 25.48 (pyrrolizine $\underline{C}H_2$-1), 50.15 (pyrrolizine $\underline{C}H_2$-3), 121.14 (phenyl $\underline{C}H$-2′ + $\underline{C}H$-6′), 128.71 (phenyl CH-3″ + CH-5″), 129.23 (phenyl CH-2″ + CH-6″), 132.08 (phenyl CH-3′ + CH-5′). MS (EI): m/z (%) 468 (M^++2, 2),

466 (M^+, 2), 357 (7), 352 (22), 311 (11), 298 (41), 297 (22), 296 (100), 268 (16), 240 (14), 232 (14), 222 (7), 205 (12), 195 (82), 184 (26), 176 (23), 156 (15), 147 (4), 139 (26), 111 (16), 104 (9), 91 (16), 77 (12). Anal. Calcd. for $C_{22}H_{16}BrClN_4O$ (467.75): C, 56.49; H, 3.45; N, 11.98; Found: C, 56.67; H, 3.83; N, 11.65.

4.1.1.6. (*E*)-*N*-(4-Bromophenyl)-7-cyano-6-((furan-2-ylmethylene)amino)-2,3-dihydro-1*H*-pyrrolizine-5-carboxamide (16)

The title compound was prepared from the reaction of compound **10a** (0.69 g, 2 mmol) with furan-2-carbaldehyde (0.23 g, 2.4 mmol) according to the general procedure A. Compound **16** was obtained as yellow solid product. IRυ_{max}/cm^{-1} 3257 (NH), 3087, 3007 (Ar C-H), 2215 (CN), 1670 (C=O), 1614, 1587, 1541 (C=C, C=N), 1459, 1417, 1394 (C-C, C-N, C-O), 547 (C-Br). ^{1}H-NMR ($CDCl_3$-500 MHz) δ (ppm): 2.52-2.58 (m, 2H, pyrrolizine CH_2-2), 3.00 (t, 2H, J = 7.6 Hz, CH_2-1), 4.49 (t, 2H, J = 7.2 Hz, CH_2-3), 6.65 (t, 1H, J = 3.6 Hz, furanyl CH-4), 7.05 (d, 1H, J = 2.6 Hz, furanyl CH-3), 7.46 (d, 2H, J = 8.4 Hz, phenyl CH-3+CH-5), 7.68 (d, 2H, J = 8.4 Hz, phenyl CH-2+CH-6), 7.73 (s, H, furanyl CH-5), 8.89 (s, H, N=CH), 11.25 (s, H, CONH). ^{13}C-NMR ($CDCl_3$, 125 MHz, δ ppm): 24.46 (pyrrolizine $\underline{C}H_2$-2), 25.37 (pyrrolizine $\underline{C}H_2$-1), 50.01 (pyrrolizine $\underline{C}H_2$-3), 113.08 (furanyl $\underline{C}$H-4), 115.95 (pyrrolizine $\underline{C}$-7), 116.13 ($\underline{C}$N), 118.16 (pyrrolizine $\underline{C}$-6), 119.36 (furanyl $\underline{C}$-3), 120.78 (phenyl $\underline{C}$-4), 120.87 (phenyl $\underline{C}$H-2 + $\underline{C}$H-6), 131.88 (phenyl $\underline{C}$H-3 + $\underline{C}$H-5), 137.91 (pyrrolizine C-5), 138.19 (pyrrolizine C-7a), 144.69 (furanyl $\underline{C}$H-5), 146.85 (N=$\underline{C}$H), 148.44 (phenyl $\underline{C}$H-1), 151.35 (furanyl $\underline{C}$-2), 158.35 ($\underline{C}$ONH). DEPT C^{135} ($CDCl_3$, 125 MHz, δ ppm): 24.47 (pyrrolizine $\underline{C}H_2$-2), 25.37 (pyrrolizine $\underline{C}H_2$-1), 50.01 (pyrrolizine $\underline{C}H_2$-3), 113.08 (furanyl $\underline{C}$-4), 119.37(furanyl $\underline{C}$-3), 120.87 (phenyl $\underline{C}$H-2 + $\underline{C}$H-6), 131.88 (phenyl $\underline{C}$H-3 + $\underline{C}$H-5), 144.70 (furanyl $\underline{C}$H-5), 146.85 (N=$\underline{C}$H). MS (EI): m/z (%) 425 (M^++3, 2), 424 (M^++2, 8), 423 (M^++1, 3), 422 (M^+, 9), 362 (4), 253 (16), 252 (100), 224 (10), 196 (8), 174 (3), 91 (5), 77 (2). Anal. Calcd. for $C_{20}H_{15}BrN_4O_2$ (423.26): C, 56.75; H, 3.57; N, 13.24; Found: C, 56.58; H, 3.12; N, 12.82.

4.1.1.7. (*E*)-*N*-(4-Bromophenyl)-7-cyano-6-((thiophen-2-ylmethylene)amino)-2,3-dihydro-1*H*-pyrrolizine-5-carboxamide (17)

The title compound was prepared from the reaction of compound **10a** (0.69 g, 2 mmol) with thiophene-2-carbaldehyde (0.27 g, 2.4 mmol) according to the general procedure A. Compound **17** was obtained as yellow solid product. IRυ_{max}/cm^{-1} 3271 (NH), 2896

(Aliphatic C-H), 2204 (CN), 1667 (C=O), 1603, 1585, 1542 (C=C, C=N), 1456, 1290 (C-C, C-N), 548 (C-Br). ^{1}H-NMR ($CDCl_3$-500 MHz, δ ppm): 2.54-2.60 (m, 2H, pyrrolizine CH_2-2), 3.05 (t, 2H, J = 7.6 Hz, pyrrolizine CH_2-1), 4.53 (t, 2H, J = 7.2 Hz, pyrrolizine CH_2-3), 7.23 (t, H, J = 3.8 Hz, thiophenyl CH-4), 7.49 (d, 2H, J = 8.3 Hz, phenyl CH-3+CH-5), 7.62 (d, H, J = 2.9 Hz, thiophenyl CH-3), 7.65 (d, H, J = 4.1 Hz, thiophenyl CH-5), 7.71 (d, 2H, J = 8.3 Hz, phenyl CH-2+CH-6), 9.31 (s, H, N=CH), 10.59 (s, H, CONH). ^{13}C-NMR ($CDCl_3$, 125 MHz, δ ppm): 24.56 (pyrrolizine $\underline{C}H_2$-2), 25.39 (pyrrolizine $\underline{C}H_2$-1), 50.21 (pyrrolizine $\underline{C}H_2$-3), 116.28 (pyrrolizine $\underline{C}$-7), 117.61 (CN), 121.25 (phenyl $\underline{C}$H-2 + $\underline{C}$H-6), 128.80 (thiophenyl $\underline{C}$H-4), 130.45 (pyrrolizine C-6), 131.60 (thiophenyl $\underline{C}$H-5), 131.96 (phenyl $\underline{C}$H-3 + $\underline{C}$H-5), 132.65 (phenyl C-4), 134.60 (thiophenyl $\underline{C}$H-3), 137.50 (pyrrolizine C-5), 138.81 (pyrrolizine C-7a), 141.84 (phenyl C-1), 148.48 (thiophenyl $\underline{C}$-2), 152.23 (N=$\underline{C}$H), 158.43 ($\underline{C}$ONH). DEPT C^{135} ($CDCl_3$, 125 MHz, δ ppm): 24.56 (pyrrolizine $\underline{C}H_2$-2), 25.39 (pyrrolizine $\underline{C}H_2$-1), 50.21 (pyrrolizine $\underline{C}H_2$-3), 121.25 (phenyl $\underline{C}$H-2 + $\underline{C}$H-6), 128.80 (thiophenyl $\underline{C}$H-4), 131.61 (thiophenyl $\underline{C}$H-5), 131.96 (phenyl $\underline{C}$H-3 + $\underline{C}$H-5), 134.60 (thiophenyl $\underline{C}$H-3), 152.23 (N=$\underline{C}$H). MS (EI): m/z (%) 425 (M^+-13, 1), 424 (M^+-14, 3), 422 (M^+-16, 4), 368 (8), 313 (6), 299 (14), 298 (31), 268 (70), 253 (19), 252 (100), 251 (5), 239 (25), 238 (12), 224 (23), 219 (17), 212 (48), 196 (17), 185 (46), 179 (86), 156 (42), 146 (29), 135 (17), 111 (38), 91 (13), 77 (24). Anal. Calcd. for $C_{20}H_{15}BrN_4OS$ (439.33): C, 54.68; H, 3.44; N, 12.75; Found: C, 55.01; H, 3.36; N, 13.21.

4.1.1.8. (*E*)-*N*-(4-Bromophenyl)-7-cyano-6-((pyridin-3-ylmethylene)amino)-2,3-dihydro-1*H*-pyrrolizine-5-carboxamide (18)

The title compound was prepared from the reaction of compound **10a** (0.69 g, 2 mmol) with pyridine-3-carbaldehyde (0.26 g, 2.4 mmol) according to the general procedure A. Compound **18** was obtained as yellow solid product. IRυ_{max}/cm^{-1} 3266 (NH), 3003 (Ar C-H), 2206 (CN), 1668 (C=O), 1611, 1591, 1542 (C=C, C=N), 1433, 1417, 1341 (C-C, C-N), 547 (C-Br). ^{1}H-NMR ($CDCl_3$-500 MHz) δ (ppm): 2.59-2.65 (m, 2H, pyrrolizine CH_2-2), 3.11 (t, 2H, J = 7.8 Hz, pyrrolizine CH_2-1), 4.57 (t, 2H, J = 7.5 Hz, pyrrolizine CH_2-3), 7.49-7.51 (m, 3H, phenyl CH-3+CH-5+ pyridinyl CH-5), 7.57 (d, 2H, J = 8.7 Hz, phenyl CH-2+CH-6), 8.21 (d, H, J = 7.6 Hz, pyridinyl CH-4), 8.81 (d, H, J = 7.0 Hz, pyridinyl CH-6), 9.18 (s, H, pyridinyl CH-2), 9.26 (s, H, N=CH), 10.51 (s, H, CONH). ^{13}C-NMR ($CDCl_3$, 125 MHz, δ ppm): 24.59 (pyrrolizine $\underline{C}H_2$-2), 25.47 (pyrrolizine $\underline{C}H_2$-1), 50.27 (pyrrolizine $\underline{C}H_2$-3), 115.96 (pyrrolizine $\underline{C}$-7), 116.67 ($\underline{C}$N), 118.23 (pyrrolizine $\underline{C}$-6), 121.17 (phenyl $\underline{C}$H-2 + $\underline{C}$H-6), 124.05 (pyridinyl CH-5), 131.06 (phenyl $\underline{C}$-4), 132.20 (phenyl $\underline{C}$H-3 +

CH-3), 135.18 (pyridinyl CH-4), 137.16 (pyridinyl C-3), 138.09 (pyrrolizine C-5), 138.65 (pyrrolizine C-7a), 148.66 (phenyl C-1), 150.09 (pyridinyl CH-2), 152.86 (pyridinyl CH-6), 157.10 (N=CH), 158.21 (CONH). DEPT C^{135} ($CDCl_3$, 125 MHz, δ ppm): 24.60 (pyrrolizine CH_2-2), 25.47 (pyrrolizine CH_2-1), 50.28 (pyrrolizine CH_2-3), 121.17 (phenyl CH-2 + CH-6), 124.06 (pyridinyl CH-5), 132.20 (phenyl CH-3 + CH-5), 135.19 (pyridinyl CH-4), 150.09 (pyridinyl CH-2), 152.86 (pyridinyl CH-6), 157.10 (N=CH). MS (EI): m/z (%) 436 (M^++3, 1), 435 (M^++2, 2), 434 (M^++1, 1), 433 (M^+, 3), 357 (10), 352 (16), 311 (8), 296 (13), 264 (16), 263 (100), 262 (19), 252 (29), 236 (36), 222 (29), 207 (17), 195 (73), 186 (24), 174 (13), 156 (18), 146 (21), 91 (30), 77 (23). Anal. Calcd. for $C_{21}H_{16}BrN_5O$ (434.29): C, 58.08; H, 3.71; N, 16.13; Found: C, 57.74; H, 3.43; N, 15.82.

4.1.1.9. (*E*)-7-Cyano-*N*-phenyl-6-(propylideneamino)-2,3-dihydro-1*H*-pyrrolizine-5-carboxamide (19)

The title compound was prepared from the reaction of compound **10b** (0.53 g, 2 mmol) with propionaldehyde (0.58 g, 10 mmol) according to the general procedure A. Compound **19** was obtained as white solid product. IRυ_{max}/cm^{-1} 3267, 3223 (NH), 3054 (Ar C-H), 2962, 2872 (Aliphatic C-H), 2214 (CN), 1668 (C=O), 1626, 1597, 1549 (C=C, C=N), 1441, 1380 (C-C, C-N). ^{1}H-NMR ($CDCl_3$, 500 MHz, δ ppm): 1.13 (t, 3H, J = 7.4 Hz, -CH_2CH_3), 2.37-2.42 (m, 2H, -CH_2CH_3), 2.50-2.55 (m, 2H, pyrrolizine CH_2-2), 2.99 (t, 2H, J = 7.6 Hz, pyrrolizine CH_2-1), 4.50 (t, 2H, J = 7.0 Hz, pyrrolizine CH_2-3), 7.10 (t, 1H, J = 7.1 Hz, phenyl CH-4), 7.35 (t, 2H, J = 7.3 Hz, phenyl CH-3 + CH-5), 7.65 (d, 2H, J = 7.8 Hz, phenyl CH-2 + CH-6), 8.77 (s, 1H, N=CH), 10.67 (s, 1H, CONH). ^{13}C-NMR ($CDCl_3$, 125 MHz, δ ppm): 11.48 (-CH_2CH_3), 22.61 (-CH_2CH_3), 24.49 (pyrrolizine CH_2-2), 25.35 (pyrrolizine CH_2-1), 50.08 (pyrrolizine CH_2-3), 116.49 (pyrrolizine C-7), 117.22 (CN), 119.68 (phenyl CH-2 + CH-6), 123.73 (phenyl CH-4), 129.03 (phenyl CH-3 + CH-5), 135.21 (pyrrolizine C-6), 138.45 (pyrrolizine C-5), 139.87 (pyrrolizine C-7a), 148.04 (phenyl C-1), 150.61 (N=CH), 158.74 (CONH). DEPT C^{135} ($CDCl_3$, 125 MHz, δ ppm): 11.48 (-CH_2CH_3), 22.61 (-CH_2CH_3), 24.49 (pyrrolizine CH_2-2), 25.35 (pyrrolizine CH_2-1), 50.08 (pyrrolizine CH_2-3), 119.68 (phenyl CH-2 + CH-6), 123.73 (phenyl CH-4), 129.04 (phenyl CH-3 + CH-5), 150.61 (N=CH). MS (EI): m/z (%) 308 ($[M+2H]^+$, 7), 307 ($[M+H]^+$, 30), 306 (M^+, 12), 277 (100), 264 (3%), 249 (4), 213 (3), 93 (3). Anal. Calcd. for $C_{18}H_{18}N_4O$ (306.36): C, 70.57; H, 5.92; N, 18.29; Found: C, 70.30; H, 5.40; N, 18.30.

4.1.1.10. (*E*)-7-Cyano-6-(propylideneamino)-*N*-(*p*-tolyl)-2,3-dihydro-1*H*-pyrrolizine-5-carboxamide (20)

The title compound was prepared from the reaction of compound **10c** (0.56 g, 2 mmol) with propionaldehyde (0.58 g, 10 mmol) according to the general procedure A. Compound **20** was obtained as white solid product. IRυ_{max}/cm^{-1} 3262, 3165 (NH), 3038 (Ar C-H), 2962, 2873 (Aliphatic C-H), 2214 (CN), 1665 (C=O), 1628, 1601, 1544 (C=C, C=N), 1480, 1380 (C-C, C-N). ^{1}H-NMR ($CDCl_3$, 500 MHz, δ ppm): 1.29 (t, 3H, J = 7.5 Hz, -CH_2CH_3), 2.23 (s, 3H, phenyl-CH_3), 2.54-4.57 (m, 2H, -CH_2CH_3), 2.66-2.74 (m, 2H, pyrrolizine CH_2-2), 3.17 (t, 2H, J = 7.5 Hz, pyrrolizine CH_2-1), 4.67 (t, 2H, J = 7.1 Hz, pyrrolizine CH_2-3), 7.31 (d, 2H, J = 8.1 Hz, phenyl CH-3 + CH-5), 7.69 (d, 2H, J = 8.1 Hz, phenyl CH-2 + CH-6), 8.93 (s, 1H, N=CH), 10.78 (s, 1H, CONH). ^{13}C-NMR ($CDCl_3$, 125 MHz, δ ppm): 11.44 (-CH_2CH_3), 20.87 (phenyl CH_3), 22.59 (-CH_2CH_3), 24.50 (pyrrolizine CH_2-2), 25.39 (pyrrolizine CH_2-1), 50.06 (pyrrolizine CH_2-3), 116.54 (pyrrolizine C-7), 117.35 (CN), 119.69 (phenyl CH-2 + CH-6), 129.52 (phenyl CH-3 + CH-5), 130.13 (phenyl C-6), 133.30 (phenyl C-5), 135.23 (phenyl C-7a), 139.72 (phenyl C-1), 147.89 (phenyl C-4), 150.46 (N=CH), 158.65 (CONH). DEPT C^{135} ($CDCl_3$, 125 MHz, δ ppm): 11.44 (-CH_2CH_3), 20.87 (phenyl-CH_3), 22.59 (-CH_2CH_3), 24.50 (pyrrolizine CH_2-2), 25.39 (pyrrolizine CH_2-1), 50.06 (pyrrolizine CH_2-3), 119.69 (phenyl CH-2 + CH-6), 129.53 (phenyl CH-3 + CH-5), 150.46 (N=CH). MS (EI): m/z (%) 361 ([M+41]$^+$, 6), 360 ([M+40]$^+$, 17), 318 ([M-2H]$^+$, 2), 291 (76), 254 (19), 198 (12), 157 (3), 107 (24), 91 (22), 77 (100). Anal. Calcd. for $C_{19}H_{20}N_4O$ (320.39): C, 71.23; H, 6.29; N, 17.49; Found: C, 70.78; H, 6.13; N, 17.62.

4.1.1.11. (*E*)-*N*-(4-Chlorophenyl)-7-cyano-6-(propylideneamino)-2,3-dihydro-1*H*-pyrrolizine-5-carboxamide (21)

The title compound was prepared from the reaction of compound **10d** (0.6 g, 2 mmol) with propionaldehyde (0.58 g, 10 mmol) according to the general procedure A. Compound **21** was obtained as white solid product. IRυ_{max}/cm^{-1} 3221, 3170 (NH), 3063 (Ar C-H), 2975, 2920 (Aliphatic C-H), 2212 (CN), 1667 (C=O), 1635, 1597, 1547 (C=C, C=N), 1493, 1310 (C-C, C-N). ^{1}H-NMR ($CDCl_3$, 500 MHz, δ ppm): 1.14 (t, 3H, J = 7.5 Hz, -CH_2CH_3), 2.37-2.44 (m, 2H, -CH_2CH_3), 2.51-2.59 (m, 2H, pyrrolizine CH_2-2), 3.03 (t, 2H, J = 7.5 Hz, pyrrolizine CH_2-1), 4.51 (t, 2H, J = 7.5 Hz, pyrrolizine CH_2-3), 7.30 (d, 2H, J = 8.7 Hz, phenyl CH-3 + CH-5), 7.60 (d, 2H, J = 8.5 Hz, phenyl CH-2 + CH-6), 8.78 (s, 1H, N=CH), 10.74 (s, 1H, CONH). ^{13}C-NMR ($CDCl_3$, 125 MHz, δ ppm): 11.47 (CH_3CH_2), 22.64 (CH_3CH_2), 24.54 (pyrrolizine CH_2-2), 25.39 (pyrrolizine CH_2-1), 50.07 (pyrrolizine CH_2-3),

116.37 (pyrrolizine C-7), 117.01 (CN), 120.85 (phenyl CH-2 + CH-6), 129.03 (phenyl CH-3 + CH-5), 130.14 (pyrrolizine C-6), 135.05 (phenyl CH-4), 137.06 (pyrrolizine C-5), 140.06 (pyrrolizine C-7a), 148.18 (phenyl CH-1), 151.00 (N=CH), 158.75 (CONH). DEPT C^{135} ($CDCl_3$, 125 MHz, δ ppm): 11.48 ($-CH_2\underline{C}H_3$), 22.65 ($-\underline{C}H_2CH_3$), 24.55 (pyrrolizine $\underline{C}H_2$-2), 25.39 (pyrrolizine $\underline{C}H_2$-1), 50.07 (pyrrolizine $\underline{C}H_2$-3), 120.85 (phenyl CH-2 + CH-6), 129.03 (phenyl CH-3 + CH-5), 151.00 (N=CH). MS (EI): m/z (%) 340 (M^+, 3), 338 ($[M-2H]^+$, 1), 311 (100), 284 (8), 254 (28), 198 (13), 127 (25), 99 (41), 77 (36). Anal. Calcd. for $C_{18}H_{17}ClN_4O$ (340.81): C, 63.44; H, 5.03; N, 16.44; Found: C, 62.88; H, 5.35; N, 16.70.

4.1.1.12. (*E*)-1-Cyano-*N*-phenyl-2-(propylideneamino)-5,6,7,8-tetrahydroindolizine-3-carboxamide (28)

The title compound was prepared from the reaction of compound **27** (0.53 g, 2 mmol) with propionaldehyde (0.58 g, 10 mmol) according to the general procedure A. Compound **28** was obtained as white solid product. IRυ_{max}/cm^{-1} 3214, 3167 (NH), 3056 (Ar C-H), 2961, 2871 (Aliphatic C-H), 2212 (CN), 1662 (C=O), 1598, 1548 (C=C, C=N), 1482, 1369 (C-C, C-N). ^{1}H-NMR ($CDCl_3$, 500 MHz, δ ppm): 1.12 (t, 3H, J = 7.5 Hz, $-CH_2C\underline{H}_3$), 1.79-1.83 (m, 2H, indolizine CH_2-7), 1.94-1.98 (m, 2H, indolizine CH_2-6), 2.25-2.29 (m, 2H, $-C\underline{H}_2CH_3$), 2.81 (t, 2H, J = 7.1 Hz, indolizine CH_2-8), 4.12-4.16 (m, 2H, J = 7.1 Hz, indolizine CH_2-5), 7.24 (t, 1H, J = 7.3 Hz, phenyl C$\underline{H}$-4), 7.38 (t, 2H, J = 7.8 Hz, phenyl C$\underline{H}$-3 + C$\underline{H}$-5), 7.63 (d, 2H, J = 7.8 Hz, phenyl C$\underline{H}$-2 + C$\underline{H}$-6), 8.61 (s, 1H, N=C$\underline{H}$), 10.47 (s, 1H, CON$\underline{H}$). ^{13}C-NMR ($CDCl_3$, 125 MHz, δ ppm): 11.32 ($-CH_2\underline{C}H_3$), 18.87 (indolizine $\underline{C}H_2$-7), 22.43 (indolizine $\underline{C}H_2$-8), 22.51 (indolizine $\underline{C}H_2$-6), 23.03 ($-\underline{C}H_2CH_3$), 45.54 (indolizine $\underline{C}H_2$-5), 114.22 (indolizine C-1), 116.53 (CN), 119.73 (phenyl CH-2 + CH-6), 123.81 (phenyl CH-4), 129.12 (phenyl CH-3 + CH-5), 136.43 (indolizine C-2), 138.22 (phenyl C-4), 140.56 (indolizine C-3), 148.26 (indolizine C-8a), 150.39 (N=CH), 158.71 (CONH). DEPT C^{135} (DMSO, 125 MHz, δ ppm): 11.32 ($-CH_2\underline{C}H_3$), 18.87 (indolizine $\underline{C}H_2$-7), 22.44 (indolizine $\underline{C}H_2$-8), 22.51 (indolizine $\underline{C}H_2$-6), 23.03 ($-\underline{C}H_2CH_3$), 45.54 (indolizine $\underline{C}H_2$-5), 119.73 (phenyl CH-2 + CH-6), 123.82 (phenyl CH-4), 129.13 (phenyl CH-3 + CH-5). MS (EI): m/z (%) 320 (M^+, 2), 319 ($[M-H]^+$, 9), 318 ($[M-2H]^+$, 13), 291 (54), 267 (32), 238 (5), 171 (5), 156 (4), 93 (47), 65 (100). Anal. Calcd. for $C_{19}H_{20}N_4O$ (320.39): C, 71.23; H, 6.29; N, 17.49; Found: C, 71.18; H, 5.84; N, 17.86.

4.1.2. General procedure (B) for the preparation of compounds 22-24 and 29

A mixture of the aniline derivatives **10b-d** or **27** (2 mmol) and propionaldehyde (0.58 g, 10 mmol) in THF (30 mL) was stirred in ice-bath for 10 min at 0 °C. Mercaptoacetic acid (1.1 g, 12 mmol) was added followed by stirring for 10 min. DCC (1g, 5 mmol) was added and the reaction mixture followed by stirring for 30 min. The temperature of the reaction mixture was allowed to rise to room temperature. The reaction mixture was stirred for additional 6 h. The reaction mixture was then filtered, the solvent was evaporated, and the solid residue was recrystallized from ethanol. The yield% and melting points of the new compounds were summarized in **Table 1**.

4.1.2.1. 7-Cyano-6-(2-ethyl-4-oxothiazolidin-3-yl)-*N*-phenyl-2,3-dihydro-1*H*-pyrrolizine-5-carboxamide (22)

The title compound was prepared from the reaction of compound **10b** (0.53g, 2 mmol) with propionaldehyde (0.58 g, 10 mmol) and mercaptoacetic acid (1.1 g, 12 mmol) according to the general procedure B. Compound **22** was obtained as white solid product. IRυ_{max}/cm^{-1} 3362 (NH), 3053 (Ar C-H), 2970, 2880 (Aliphatic C-H), 2228 (CN), 1693, 1662 (C=O), 1597, 1536 (C=C, C=N), 1460, 1398 (C-C, C-N). ^{1}H-NMR (DMSO-d_6, 500 MHz, δ ppm): 0.89 (t, 3H, J = 7.3, $CH_2C\underline{H}_3$), 1.59-1.67 (m, 1H, -C$\underline{H}_2CH_3$), 1.80-1.84 (m, 1H, -C$\underline{H}_2CH_3$), 2.45-2.51 (m, 2H, pyrrolizine C$\underline{H}_2$-2), 3.04 (t, 2H, J = 7.4, pyrrolizine C$\underline{H}_2$-1), 3.74-3.83 (m, 2H, thiazolidinone C$\underline{H}_2$), 4.26-4.37 (m, 2H, pyrrolizine C$\underline{H}_2$-3), 5.11 (dd, 1H, thiazolidinone C$\underline{H}$-2), 7.12 (t, 1H, J = 7.4 Hz, phenyl CH-4), 7.36 (t, 2H, J = 7.8 Hz, phenyl CH-3 + CH-5), 7.62 (t, 2H, J = 8.0 Hz, phenyl CH-2 + CH-6), 9.61 (s, 1H, CONH). ^{13}C-NMR (DMSO, 125 MHz, δ ppm): 8.87 ($\underline{C}H_3CH_2$), 24.99 (pyrrolizine $\underline{C}H_2$-2), 25.74 (pyrrolizine $\underline{C}H_2$-1), 28.61 ($CH_3\underline{C}H_2$), 31.59 (thiazolidinone $\underline{C}H_2$), 49.85 (pyrrolizine $\underline{C}H_2$-3), 65.21 (thiazolidinone $\underline{C}$H-1), 85.23 (pyrrolizine $\underline{C}$-7), 114.66 ($\underline{C}$N), 120.44 (phenyl $\underline{C}$H-2 + $\underline{C}$H-6), 120.94 (pyrrolizine $\underline{C}$-5), 124.59 (phenyl $\underline{C}$H-4), 126.42 (pyrrolizine $\underline{C}$-7a), 129.33 (phenyl $\underline{C}$H-3 + $\underline{C}$H-5), 138.60 (phenyl $\underline{C}$-1), 146.68 (pyrrolizine $\underline{C}$-6), 157.40 (phenyl NH$\underline{C}$=O), 172.27 (thiazolidinone $\underline{C}$=O). DEPT C^{135} (DMSO, 125 MHz, δ ppm): 8.87 ($\underline{C}H_3CH_2$), 24.99 (pyrrolizine $\underline{C}H_2$-2), 25.74 (pyrrolizine $\underline{C}H_2$-1), 28.61 ($CH_3\underline{C}H_2$), 31.59 (thiazolidinone $\underline{C}H_2$), 49.85 (pyrrolizine $\underline{C}H_2$-3), 65.21 (thiazolidinone $\underline{C}$H-2), 120.44 (phenyl $\underline{C}$H-2 + $\underline{C}$H-6), 124.59 (phenyl $\underline{C}$H-4), 129.33 (phenyl $\underline{C}$H-3 + $\underline{C}$H-5). MS (EI): m/z (%) 383 ([M+3H]$^+$, 2), 382 ([M+2H]$^+$, 8), 381 ([M+H]$^+$, 31), 380 (M$^+$, 100), 351 (9), 305 (7), 288 (15), 93 (5), 77

(8). Anal. Calcd. for $C_{20}H_{20}N_4O_2S$ (380.46): C, 63.14; H, 5.30; N, 14.73; Found: C, 62.88; H, 5.59; N, 15.12.

4.1.2.2. 7-Cyano-6-(2-ethyl-4-oxothiazolidin-3-yl)-*N*-(*p*-tolyl)-2,3-dihydro-1*H*-pyrrolizine-5-carboxamide (23)

The title compound was prepared from the reaction of compound **10c** (0.56 g, 2 mmol) with propionaldehyde (0.58 g, 10 mmol) and mercaptoacetic acid (1.1 g, 12 mmol) according to the general procedure B. Compound **23** was obtained as white solid product. IRυ_{max}/cm^{-1} 3371 (NH), 3101 (Ar C-H), 2998, 2876 (Aliphatic C-H), 2228 (CN), 1696, 1664 (C=O), 1596 (C=C, C=N), 1423, 1321 (C-C, C-N). ^{1}H-NMR (DMSO-d_6, 500 MHz, δ ppm): 0.88 (t, 3H, J = 7.2, -CH_2C$\underline{H}_3$), 1.59-1.64 1.62 (m, 1H, CH_3-C$\underline{H}_2$), 1.78-1.82 (m, 1H, -C$\underline{H}_2$$CH_3$), 2.27 (s, 3H, phenyl-C$\underline{H}_3$), 2.46-2.51 (m, 2H, pyrrolizine C$\underline{H}_2$-2), 3.04 (t, 2H, J = 7.3, pyrrolizine C$\underline{H}_2$-1), 3.74-3.83 (m, 2H, thiazolidinone C$\underline{H}_2$), 4.25-4.37 (m, 2H, pyrrolizine C$\underline{H}_2$-3), 5.10 (d, 1H, J = 6.0, thiazolidinone C$\underline{H}$-2), 7.16 (d, 2H, J = 8.1 Hz, phenyl CH-3 + CH-5), 7.51 (d, 2H, J = 8.2 Hz, phenyl CH-2 + CH-6), 9.54 (s, 1H, CONH). ^{13}C-NMR (DMSO, 125 MHz, δ ppm): 8.83 ($\underline{C}H_3CH_2$), 20.95 (phenyl CH_3), 24.98 (pyrrolizine $\underline{C}H_2$-2), 25.74 (pyrrolizine $\underline{C}H_2$-1), 28.59 ($CH_3\underline{C}H_2$), 31.60 (thiazolidinone $\underline{C}H_2$), 49.81 (pyrrolizine $\underline{C}H_2$-3), 65.18 (thiazolidinone $\underline{C}$H-1), 85.14 (pyrrolizine $\underline{C}$-7), 114.69 ($\underline{C}$N), 120.39 (phenyl $\underline{C}$H-2 + $\underline{C}$H-6), 121.03 (pyrrolizine $\underline{C}$-5), 126.22 (pyrrolizine $\underline{C}$-7a), 129.70 (phenyl $\underline{C}$H-3 + $\underline{C}$H-5), 133.66 (phenyl $\underline{C}$-1), 136.09 (phenyl $\underline{C}$-4), 146.59 (pyrrolizine $\underline{C}$-6), 157.22 (phenyl NH$\underline{C}$=O), 172.28 (thiazolidinone $\underline{C}$=O). DEPT C^{135} (DMSO, 125 MHz, δ ppm): 8.84 ($\underline{C}H_3CH_2$), 20.95 (phenyl CH_3), 24.98 (pyrrolizine $\underline{C}H_2$-2), 25.75 (pyrrolizine $\underline{C}H_2$-1), 28.59 ($CH_3\underline{C}H_2$), 31.60 (thiazolidinone $\underline{C}H_2$), 49.81 (pyrrolizine $\underline{C}H_2$-3), 65.19 (thiazolidinone $\underline{C}$H-2), 120.39 (phenyl $\underline{C}$H-2 + $\underline{C}$H-6), 129.70 (phenyl $\underline{C}$H-3 + $\underline{C}$H-5). MS (EI): m/z (%) 397 ([M+3H]$^+$, 2), 396 ([M+2H]$^+$, 8), 395 ([M+H]$^+$, 25), 394 (M$^+$, 100), 393 ([M-H]$^+$, 9), 365 (4), 319 (3), 288 (11), 107 (3), 77 (5). Anal. Calcd. for $C_{21}H_{22}N_4O_2S$ (394.49): C, 63.94; H, 5.62; N, 14.20; Found: C, 64.05; H, 5.24; N, 14.55.

4.1.2.3. *N*-(4-Chlorophenyl)-7-cyano-6-(2-ethyl-4-oxothiazolidin-3-yl)-2,3-dihydro-1*H*-pyrrolizine-5-carboxamide (24)

The title compound was prepared from the reaction of compound **10d** (0.6 g, 2 mmol) with propionaldehyde (0.58 g, 10 mmol) and mercaptoacetic acid (1.1 g, 12 mmol) according to the general procedures B. Compound **24** was obtained as white solid product. IRυ_{max}/cm^{-1} 3262 (NH), 2973, 2934 (Aliphatic C-H), 2229 (CN), 1698, 1666 (C=O), 1594, 1529

(C=C, C=N), 1492, 1315 (C-C, C-N). ^{1}H-NMR (DMSO-d_6, 500 MHz, δ ppm): 0.89 (t, 3H, J = 7.2, -CH_2CH_3), 1.60-1.66 (m, 1H, -CH_2CH_3), 1.78-1.83 (m, 1H, CH_3-CH_2), 2.45-2.51 (m, 2H, pyrrolizine CH_2-2), 3.04 (t, 2H, J = 7.3, pyrrolizine CH_2-1), 3.71-3.82 (m, 2H, thiazolidinone CH_2), 4.29-4.34 (m, 2H, pyrrolizine CH_2-3), 5.09 (d, 1H, J = 7.4, thiazolidinone CH-2), 7.41 (d, 2H, J = 8.2 Hz, phenyl CH-3 + CH-5), 7.66 (d, 2H, J = 8.3 Hz, phenyl CH-2 + CH-6), 9.78 (s, 1H, CONH). ^{13}C-NMR (DMSO, 125 MHz, δ ppm): 8.89 (CH_3CH_2), 24.99 (pyrrolizine CH_2-2), 25.73 (pyrrolizine CH_2-1), 28.65 (CH_3CH_2), 31.59 (thiazolidinone CH_2), 49.87 (pyrrolizine CH_2-3), 65.20 (thiazolidinone CH-1), 85.42 (pyrrolizine C-7), 114.69 (CN), 120.58 (pyrrolizine C-5), 122.08 (phenyl CH-2 + CH-6), 126.82 (pyrrolizine C-7a), 128.19 (phenyl C-4), 129.19 (phenyl CH-3 + CH-5), 137.62 (phenyl C-1), 146.79 (pyrrolizine C-6), 157.49 (phenyl NHC=O), 172.13 (thiazolidinone C=O). DEPT C^{135} (DMSO, 125 MHz, δ ppm): 8.89 (CH_3CH_2), 24.99 (pyrrolizine CH_2-2), 25.73 (pyrrolizine CH_2-1), 28.65 (CH_3CH_2), 31.59 (thiazolidinone CH_2), 49.87 (pyrrolizine CH_2-3), 65.20 (thiazolidinone CH-2), 122.08 (phenyl CH-2 + CH-6), 129.19 (phenyl CH-3 + CH-5). MS (EI): m/z (%) 417 ($[M+3H]^+$, 10), 416 ($[M+2H]^+$, 40), 415 ($[M+H]^+$, 27), 414 (M^+, 100), 385 (14), 339 (23), 311 (23), 288 (85), 258 (8), 232 (3), 186 (7), 127 (9), 99 (11). Anal. Calcd. for $C_{20}H_{19}ClN_4O_2S$ (414.91): C, 57.90; H, 4.62; N, 13.50; Found: C, 58.31; H, 4.12; N, 13.96.

4.1.2.4. 1-Cyano-2-(2-ethyl-4-oxothiazolidin-3-yl)-*N*-phenyl-5,6,7,8-tetrahydroindolizine-3-carboxamide (29)

The title compound was prepared from the reaction of compound **27** (0.53 g, 2 mmol) with propionaldehyde (0.58 g, 10 mmol) and mercaptoacetic acid (1.1 g, 12 mmol) according to the general procedures B. Compound **29** was obtained as white solid product. IRυ_{max}/cm^{-1} 3295 (NH), 3061, 3021 (Ar C-H), 2937, 2870 (Aliphatic C-H), 2223 (CN), 1686, 1657 (C=O), 1601, 1545 (C=C, C=N), 1424, 1342 (C-C, C-N). ^{1}H-NMR (DMSO-d_6, 500 MHz, δ ppm): 0.86 (t, 3H, J = 7.2, -CH_2CH_3), 1.56-1.61 (m, 1H, -CH_2CH_3), 1.77-1.84 (m, 3H, -CH_2CH_3 + indolizine CH_2-7), 1.91-1.95 (m, 2H, indolizine CH_2-6), 2.89 (t, 2H, J = 6.2, indolizine CH_2-8), 3.73-3.80 (m, 2H, thiazolidinone CH_2), 4.07-4.20 (m, 2H, indolizine CH_2-5), 5.05 (d, 1H, J = 7.2, thiazolidinone CH-2), 7.13 (t, 1H, J = 7.4 Hz, phenyl CH-4), 7.35 (t, 2H, J = 7.8 Hz, phenyl CH-3 + CH-5), 7.60 (d, 2H, J = 7.9 Hz, phenyl CH-2 + CH-6), 9.86 (s, 1H, CONH). ^{13}C-NMR (DMSO, 125 MHz, δ ppm): 8.60 (CH_3CH_2), 18.90 (indolizine CH_2-7), 22.47 (indolizine CH_2-8), 22.55 (indolizine CH_2-6), 28.53 (CH_3-CH_2), 31.65 (thiazolidinone CH_2), 45.69 (indolizine CH_2-5), 65.09 (thiazolidinone CH-1), 88.71 (indolizine C-1), 114.48

(CN), 120.26 (phenyl CH-2 + CH-6), 122.83 (indolizine C-3), 124.64 (indolizine C-8a), 124.70 (phenyl CH-4), 129.38 (phenyl CH-3 + CH-5), 138.57 (phenyl C-1), 140.64 (indolizine C-2), 157.54 (phenyl NHC=O), 172.29 (thiazolidinone C=O). DEPT C^{135} (DMSO, 125 MHz, δ ppm): 8.60 (CH_3CH_2), 18.90 (indolizine CH_2-7), 22.47 (indolizine CH_2-8), 22.55 (indolizine CH_2-6), 28.53 (CH_3-CH_2), 31.65 (thiazolidinone CH_2), 45.69 (indolizine CH_2-5), 65.09 (thiazolidinone CH-2), 120.26 (phenyl CH-2 + CH-6), 124.70 (phenyl CH-4), 129.38 (phenyl CH-3 + CH-5). MS (EI): m/z (%) 397 ($[M+3H]^+$, 2), 396 ($[M+2H]^+$, 8), 395 ($[M+H]^+$, 27), 394 (M^+, 100), 393 ($[M-H]^+$, 13), 365 (15), 347 (6), 319 (8), 302 (52), 93 (8), 77 (9). Anal. Calcd. for $C_{21}H_{22}N_4O_2S$ (394.49): C, 63.94; H, 5.62; N, 14.20; Found: C, 64.39; H, 5.60; N, 14.01.

4.2. Biological Evaluation

4.2.1. Cytotoxicity activity

4.2.1.1. Cell culture

Three human cancer (breast MCF-7, ovarian A2780 and colon HT29) and one normal (foetal lung fibroblast, MRC5) cell lines of the American Type Culture Collection (ATCC, Manassas, VA) were used in the MTT assay. Dulbecco's modified Eagles medium (DMEM) supplemented with 10% foetal bovine serum (FBS; Gibco) was used as the culture media. Both cancer and normal cell lines were cultured according to our previous report [21].

4.2.1.2. Cytotoxicity assay

Cytotoxic activity of the newly prepared compounds was determined by MTT assay against the four selected cell lines, according to our previous report [43]. After treatment with the test compound for 72 h, the absorbance of the reduced MTT was determined using microplate reader (570 nm). The results were presented in **Tables 2-4**.

4.2.2. Anti-inflammatory activity

4.2.2.1. *In vitro* COXs inhibition assay

The inhibitory effects of the tested compounds against both COX-1 (human, Item No. 701070) and COX-2 (human, Item No. 701080) enzymes was measured using COX inhibitor screening assay kit provided from Cayman Chemicals. The assay was performed following manufacturer's instructions and as previously report [46]. The results were presented as IC_{50} values ± SEM in **Table 5**.

4.2.2.2. *In vivo* anti-inflammatory activity

The anti-inflammatory effect of compound **12**, **14**, **16**, and **24** was evaluated using the rat paw edema method described by Winter *et al.* [47]. Both male and female adult albino rats (100-140 g) were used. The procedures of this study including the animal work was approved by the ethical committee (college of pharmacy, Umm Al-Qura University). The test compounds (0.5 mmol), celecoxib (25 mg/kg), and indomethacin (15 mg/kg) were given orally. The procedures were completed as described in our previous report [48]. The results were presented in **Table 6**.

4.2.3. Kinase inhibitory activity

4.2.3.1. Kinase profiling test

The kinase inhibitory activity of compound **12**, **19** and **20** and imatinib (reference drug) was evaluated using the radiolabeled ATP determination method (KINEXUS Bioinformatics Corporation, Vancouver, BC, Canada). The test was performed as described in our previous report [21]. The inhibitory activity of the selected kinases were presented in **Table 7**.

4.2.3.2. CDK2 inhibitory assay

CDK2 inhibitory activity by compounds **12**, **19**, and **22** was determined *in vitro* using ADP-Glo assay (Promega).The assay was done according to manufacturer's instructions and as described in the previous report [52]. CDK2 was incubated with the substrate, test compounds (dissolved in 5% DMSO) and ATP in kinase buffer. After the incubation, ADP-Glo Reagent was added to stop kinase reaction and to remove the unreacted ATP. Kinase detection reagent was added to convert ADP into equivalent amount of ATP. The later was converted to luminescent which correlate to kinases activity. The IC_{50} values were obtained from the plot of kinase activity versus concentration of test compounds. The results were presented in **Table 8**.

4.2.4. Cell cycle analysis

The effect of compounds **12**, **14**, **16** and **22** on cell cycle perturbation of MCF-7 cells was analyzed using flow cytometric analysis. The flow cytometer (BC, FC500) was used to analyze the propidium iodide-stained cells according to our previous reports [21]. Results were presented in **Table 9**.

4.2.5. Annexin V-FITC/PI staining assay

Annexin V-FITC/PI staining assay was used to measure the effect of compounds **12**, **14**, **16** and **22** on apoptotic events in MCF-7 cells. The assay was performed following our previous report [43]. After treatment of with test compounds, cells were analyzed by flow cytometry. Early and late apoptotic/necrotic cells were differentiated from viable cells by Annexin V (x axis) and PI staining (y axis), **Figs. 8** and (Fig. S115, supplementary data).

4.3. Molecular docking study

The pdb files of COX-1 (pdb code: 1EQG) [56], COX-2 (pdb code: 1CX2) [59], CDK2 (pdb code: 3TNW) [61], Aurora A (pdb code: 3E5A) [62], BRAF (pdb code: 4RZV) [63] and EGFR (pdb code: 1M17) [64] were downloaded from protein data bank (http://www.rcsb.org/pdb). Docking studies were done using AutoDock 4.2 [54]. The preparation of ligands, enzymes, affinity map, grid and docking parameter files was done following our previous reports [21,57,58]. The results including binding free energy (ΔG_b) and inhibition constants (K_i) were represented in **Tables 10-12**. The 2D/3D binding modes (**Figs. 9** and **10**) of the tested compounds into the active site of the selected enzymes were visualized by LigPlot$^+$ [65] and Discovery Studio Visualizer (v16.1.0.15350) [55]. Additionally, the 2/3D binding interactions of compounds **11-13, 19-22**, **24**, and **28** with the relevant enzymes were presented in supplementary data (Figures S116-119).

Acknowledgement

This work was funded by National Science, Technology and Innovation Plan (MAARIFAH), King Abdulaziz City for Science and Technology (KACST), Kingdom of Saudi Arabia, grant number (12-MED2304-10-R).

Supplementary data

Supplementary data including spectral data (IR, Mass, ^{1}H-NMR, ^{13}C-NMR DEPT 135 spectra) of the final compounds was provided with this manuscript (**Fig. S1-S112**).

Conflict of Interest

Authors declared that there is no conflict of interest and have approved the article.

5. References

1. R. Bayat Mokhtari, T.S. Homayouni, N. Baluch, E. Morgatskaya, S. Kumar, B. Das, H. Yeger, Combination therapy in combating cancer, Oncotarget. 8 (2017) 38022–38043. doi:10.18632/oncotarget.16723.
2. S.-H. Chen, G. Lahav, Two is better than one; toward a rational design of combinatorial therapy, Curr. Opin. Struct. Biol. 41 (2016) 145–150. doi:10.1016/j.sbi.2016.07.020.
3. M. Leary, S. Heerboth, K. Lapinska, S. Sarkar, Sensitization of Drug Resistant Cancer Cells: A Matter of Combination Therapy, Cancers (Basel). 10 (2018) 483. doi:10.3390/cancers10120483.
4. R.P. Riechelmann, I.F. Tannock, L. Wang, E.D. Saad, N.A. Taback, M.K. Krzyzanowska, Potential drug interactions and duplicate prescriptions among cancer patients, J. Natl. Cancer Inst. 99 (2007) 592–600. doi:10.1093/jnci/djk130.
5. N.M. Raghavendra, D. Pingili, S. Kadasi, A. Mettu, S.V.U.M. Prasad, Dual or multi-targeting inhibitors: The next generation anticancer agents, Eur. J. Med. Chem. 143 (2018) 1277–1300. doi:10.1016/j.ejmech.2017.10.021.
6. J.G. Monzon, J. Dancey, Chapter 11 Combination Agents Versus Multi-Targeted Agents – Pros and Cons, in: Des. Multi-Target Drugs, The Royal Society of Chemistry, 2012: pp. 155–180. doi:10.1039/9781849734912-00155.
7. A.A. Antolin, P. Workman, J. Mestres, B. Al-Lazikani, Polypharmacology in Precision Oncology: Current Applications and Future Prospects, Curr. Pharm. Des. 22 (2016) 6935–6945. doi:10.2174/1381612822666160923115828.
8. C. Ma, S. Wei, Y. Song, T790M and acquired resistance of EGFR TKI: a literature review of clinical reports, J. Thorac. Dis. 3 (2011) 10–18. doi:10.3978/j.issn.2072-1439.2010.12.02.

9. Q. Jiao, L. Bi, Y. Ren, S. Song, Q. Wang, Y. Wang, Advances in studies of tyrosine kinase inhibitors and their acquired resistance, Mol. Cancer. 17 (2018) 36. doi:10.1186/s12943-018-0801-5.
10. F.R. Balkwill, A. Mantovani, Cancer-related inflammation: common themes and therapeutic opportunities., Semin. Cancer Biol. 22 (2012) 33–40. doi:10.1016/j.semcancer.2011.12.005.
11. G.J. Tsioulias, M.F. Go, B. Rigas, NSAIDs and Colorectal Cancer Control: Promise and Challenges, Curr. Pharmacol. Reports. 1 (2015) 295–301. doi:10.1007/s40495-015-0042-x.
12. L.M. Coussens, Z. Werb, Inflammation and cancer, Nature. 420 (2002) 860–867. doi:10.1038/nature01322.
13. A.J. Schetter, N.H.H. Heegaard, C.C. Harris, Inflammation and cancer: interweaving microRNA, free radical, cytokine and p53 pathways., Carcinogenesis. 31 (2010) 37–49. doi:10.1093/carcin/bgp272.
14. R.E. Harris, B.C. Casto, Z.M. Harris, Cyclooxygenase-2 and the inflammogenesis of breast cancer., World J. Clin. Oncol. 5 (2014) 677–692. doi:10.5306/wjco.v5.i4.677.
15. H. Sun, X. Zhang, D. Sun, X. Jia, L. Xu, Y. Qiao, Y. Jin, COX-2 expression in ovarian cancer: an updated meta-analysis., Oncotarget. 8 (2017) 88152–88162. doi:10.18632/oncotarget.21538.
16. A.T. Koki, J.L. Masferrer, Celecoxib: a specific COX-2 inhibitor with anticancer properties., Cancer Control. 9 (2002) 28–35. doi:10.1177/107327480200902S04.
17. T. Kitamura, T. Kawamori, N. Uchiya, M. Itoh, T. Noda, M. Matsuura, T. Sugimura, K. Wakabayashi, Inhibitory effects of mofezolac, a cyclooxygenase-1 selective inhibitor, on intestinal carcinogenesis., Carcinogenesis. 23 (2002) 1463–1466. https://doi.org/10.1093/carcin/23.9.1463.
18. E. Gurpinar, W.E. Grizzle, G.A. Piazza, NSAIDs inhibit tumorigenesis, but how?, Clin. Cancer Res. 20 (2014) 1104–1113. doi:10.1158/1078-0432.CCR-13-1573.
19. D.A. Madrigal, C.H. Escalante, G.A. Gutiérrez-Rebolledo, J.M. Cristobal-Luna, O. Gómez-García, R.I. Hernández-Benitez, A.L. Esquivel-Campos, S. Pérez-Gutiérrez, G.A. Chamorro-Cevallos, F. Delgado, J. Tamariz, Synthesis and highly potent anti-inflammatory activity of licofelone- and ketorolac-based 1-arylpyrrolizin-3-ones, Bioorg. Med. Chem. 27 (2019) 115053. doi: https://doi.org/10.1016/j.bmc.2019.115053.

20. A.M. Gouda, A.H. Abdelazeem, A.N. Abdalla, M. Ahmed, Pyrrolizine-5-carboxamides: exploring the impact of various substituents on anti-inflammatory and anticancer activities, Acta Pharm 68 (2018) 251–273. https ://doi.org/10.2478/acph-2018-0026.
21. A.M. Gouda, A.H. Abdelazeem, H.A. Omar, A.N. Abdalla, M.A.S. Abourehab, H.I. Ali, Pyrrolizines: Design, synthesis, anticancer evaluation and investigation of the potential mechanism of action, Bioorg. Med. Chem. 25 (2017) 5637–5651. doi:https://doi.org/10.1016/j.bmc.2017.08.039.
22. S. Tavolari, A. Munarini, G. Storci, S. Laufer, P. Chieco, T. Guarnieri, The decrease of cell membrane fluidity by the non-steroidal anti-inflammatory drug Licofelone inhibits epidermal growth factor receptor signalling and triggers apoptosis in HCA-7 colon cancer cells, Cancer Lett. 321 (2012) 187–194. doi:10.1016/j.canlet.2012.02.003.
23. J. Hirst, H.B. Pathak, S. Hyter, Z.Y. Pessetto, T. Ly, S. Graw, D.C. Koestler, A.J. Krieg, K.F. Roby, A.K. Godwin, Licofelone Enhances the Efficacy of Paclitaxel in Ovarian Cancer by Reversing Drug Resistance and Tumor Stem-like Properties, Cancer Res. 78 (2018) 4370–4385. doi:10.1158/0008-5472.CAN-17-3993.
24. C. Kurkjian, N.B. Janakiram, S. Guruswamy, C. V Rao, H. Ozer, The effects of licofelone, a dual lipoxygenase and cyclooxygenase inhibitor, with and without rosiglitazone in human MCF-7 and MDA-MB-231 breast cancer cells, J. Clin. Oncol. 25 (2007) 1537. doi:10.1200/jco.2007.25.18_suppl.1537.
25. C. V Rao, N.B. Janakiram, V. Madka, V. Devarkonda, M. Brewer, L. Biddick, S. Lightfoot, V.E. Steele, A. Mohammed, Simultaneous targeting of 5-LOX-COX and EGFR blocks progression of pancreatic ductal adenocarcinoma, Oncotarget. 6 (2015) 33290–33305. doi:10.18632/oncotarget.5396.
26. X. Hu, L.-W. Wu, X. Weng, N.-M. Lin, C. Zhang, Synergistic antitumor activity of aspirin and erlotinib: Inhibition of p38 enhanced aspirin plus erlotinib-induced suppression of metastasis and promoted cancer cell apoptosis, Oncol. Lett. 16 (2018) 2715–2724. doi:10.3892/ol.2018.8956.
27. Y.X. Li, J. Le Wang, M. Gao, H. Tang, R. Gui, Y.F. Fu, Celecoxib-erlotinib combination delays growth and inhibits angiogenesis in EGFR-mutated lung cancer, Am. J. Cancer Res. 6 (2016) 1494–1510.
28. N.J. Samadder, D. Neklason, K. Boucher, K. Priyanka, K. Byrne, W. Samowitz, T. Greene, L.M. Pappas, S. Tavtigian, M.W. Done, T. Berry, L. Smith, D. Sample, R.W. Burt, S.K. Kuwada, Effect of COX and EGFR Inhibition on Colorectal Neoplasia in

Familial Adenomatous Polyposis: A Randomized Placebo controlled Trial, Gastroenterology. 152 (2017) S140. doi:10.1016/S0016-5085(17)30797-7.

29. R. Fu, Y. Sun, W. Sheng, D. Liao, Designing multi-targeted agents: An emerging anticancer drug discovery paradigm, Eur. J. Med. Chem. 136 (2017) 195–211. doi:10.1016/j.ejmech.2017.05.016.
30. W. Zheng, Y. Zhao, Q. Luo, Y. Zhang, K. Wu, F. Wang, Multi-Targeted Anticancer Agents, Curr. Top. Med. Chem. 17 (2017) 3084–3098. doi:10.2174/1568026617666170707124126.
31. P. Traxler, P. Furet, Strategies toward the Design of Novel and Selective Protein Tyrosine Kinase Inhibitors, Pharmacol. Ther. 82 (1999) 195–206. doi:10.1016/S0163-7258(98)00044-8.
32. C.M. Richardson, C.L. Nunns, D.S. Williamson, M.J. Parratt, P. Dokurno, R. Howes, J. Borgognoni, M.J. Drysdale, H. Finch, R.E. Hubbard, P.S. Jackson, P. Kierstan, G. Lentzen, J.D. Moore, J.B. Murray, H. Simmonite, A.E. Surgenor, C.J. Torrance, Discovery of a potent CDK2 inhibitor with a novel binding mode, using virtual screening and initial, structure-guided lead scoping, Bioorg. Med. Chem. Lett. 17 (2007) 3880–3885. doi:10.1016/j.bmcl.2007.04.110.
33. A. Ermoli, A. Bargiotti, M.G. Brasca, A. Ciavolella, N. Colombo, G. Fachin, A. Isacchi, M. Menichincheri, A. Molinari, A. Montagnoli, A. Pillan, S. Rainoldi, F.R. Sirtori, F. Sola, S. Thieffine, M. Tibolla, B. Valsasina, D. Volpi, C. Santocanale, E. Vanotti, Cell division cycle 7 kinase inhibitors: 1H-pyrrolo[2,3-b]pyridines, synthesis and structure-activity relationships, J. Med. Chem. 52 (2009) 4380–4390. doi:10.1021/jm900248g.
34. F. Kilchmann, M.J. Marcaida, S. Kotak, T. Schick, S.D. Boss, M. Awale, P. Gönczy, J.-L. Reymond, Discovery of a Selective Aurora A Kinase Inhibitor by Virtual Screening, J. Med. Chem. 59 (2016) 7188–7211. doi:10.1021/acs.jmedchem.6b00709.
35. C.J.R. Bataille, M.B. Brennan, S. Byrne, S.G. Davies, M. Durbin, O. Fedorov, K.V.M. Huber, A.M. Jones, S. Knapp, G. Liu, A. Nadali, C.E. Quevedo, A.J. Russell, R.G. Walker, R. Westwood, G.M. Wynne, Thiazolidine derivatives as potent and selective inhibitors of the PIM kinase family, Bioorg. Med. Chem. 25 (2017) 2657–2665. doi:https://doi.org/10.1016/j.bmc.2017.02.056.
36. P.-C. Lv, C.-F. Zhou, J. Chen, P.-G. Liu, K.-R. Wang, W.-J. Mao, H.-Q. Li, Y. Yang, J. Xiong, H.-L. Zhu, Design, synthesis and biological evaluation of thiazolidinone derivatives as potential EGFR and HER-2 kinase inhibitors, Bioorg. Med. Chem. 18 (2010) 314–319. doi:https://doi.org/10.1016/j.bmc.2009.10.051.

37. M.M.M. El-Miligy, H.A. Abd El Razik, M.M. Abu-Serie, Synthesis of piperazine-based thiazolidinones as VEGFR2 tyrosine kinase inhibitors inducing apoptosis, Future Med. Chem. 9 (2017) 1709–1729. doi:10.4155/fmc-2017-0072.
38. M.T. Elsaady, A.M. Gouda, F.H. Edrees, N.M.A. Gawad, synthesis and biological evaluation of some novel Schiff base derivatives as potential anticancer agents, J Chem. Pharm. Res. 8 (2016) 273–282.
39. K.M. Attallah, A.M. Gouda, I.T. Ibrahim, L. Abouzeid, Design, synthesis, 99mTc labeling, and biological evaluation of a novel pyrrolizine derivative as potential anti-inflammatory agent, Radiochemistry. 59 (2017) 630–638. doi:10.1134/S10663622170600121.
40. M.Y. Ebeid, S. M.A. El. Moghazy, M.M. Hanna, F.A. Romeih, F.F. Barsoum, Synthesis and anti-HIV activity of some 6,7-dihydro-5H-pyrrolizine-3-carboxamide, 5,6,7,8-tetrahydroindolizine-3-carboxamide, 1-thioxo-1,2,3,5, 6,7,8,9,10,11-decahydro-pyrimido[1,6-a]azonine-4-carbonitrile and 6-thioxo-1,2,5,6,8,9,10,11,12,13,14,14a-dodecahydropyrimido[4′,5′:4,5]pyrimido[1,6-a]azonine-1-one derivatives, Bull. Fac. Pharm. (Cairo Univ.) 3 (1997) 171-83.
41. S.E. Abbas, F.M. Awadallah, N.A. Ibrahim, A.M. Gouda, B.A. Shehata, Design, synthesis and preliminary evaluation of some novel [1,4]diazepino [5,6-b]pyrrolizine and 6-(2-oxopyrrolidino)-1Hpyrrolizine derivatives as anticonvulsant agents, Med. Chem. Res. 20 (2011) 1015–1023. doi:10.1007/s00044-010-9429-8.
42. S.W. Rowlinson, B.C. Crews, D.C. Goodwin, C. Schneider, J.K. Gierse, L.J. Marnett, Spatial requirements for 15-(R)-hydroxy-5Z,8Z,11Z, 13E-eicosatetraenoic acid synthesis within the cyclooxygenase active site of murine COX-2. Why acetylated COX-1 does not synthesize 15-(R)-hete., J. Biol. Chem. 275 (2000) 6586–6591. doi:10.1074/jbc.275.9.6586.
43. W.H. Malki, A.M. Gouda, H.E.A. Ali, R. Al-Rousan, D. Samaha, A.N. Abdalla, J. Bustamante, Z.Y. Abd Elmageed, H.I. Ali, Structural-based design, synthesis, and antitumor activity of novel alloxazine analogues with potential selective kinase inhibition, Eur. J. Med. Chem. 152 (2018) 31–52. doi:https://doi.org/10.1016/j.ejmech.2018.04.029.
44. M. Ghoncheh, Z. Pournamdar, H. Salehiniya, Incidence and Mortality and Epidemiology of Breast Cancer in the World, Asian Pac. J. Cancer Prev. 17 (2016) 43–46. doi:10.7314/apjcp.2016.17.s3.43.

45. A. Belal, A.M. Gouda, A.S. Ahmed, N.M. Abdel Gawad, Synthesis of novel indolizine, diazepinoindolizine and Pyrimidoindolizine derivatives as potent and selective anticancer agents, Res. Chem. Intermed. 41 (2015) 9687–9701. doi:10.1007/s11164-015-1958-9.
46. S.-Z. Ren, Z.-C. Wang, D. Zhu, X.-H. Zhu, F.-Q. Shen, S.-Y. Wu, J.-J. Chen, C. Xu, H.-L. Zhu, Design, synthesis and biological evaluation of novel ferrocene-pyrazole derivatives containing nitric oxide donors as COX-2 inhibitors for cancer therapy, Eur. J. Med. Chem. 157 (2018) 909–924. doi:https://doi.org/10.1016/j.ejmech.2018.08.048.
47. C.A. Winter, E.A. Risley, G.W. Nuss, Carrageenin-induced edema in hind paw of the rat as an assay for antiiflammatory drugs, Proc. Soc. Exp. Biol. Med. 111 (1962) 544–547. Doi: 10.3181/00379727-111-27849.
48. A.M. Gouda, H.I. Ali, W.H. Almalki, M.A. Azim, M.A.S. Abourehab, A.H. Abdelazeem, Design, Synthesis, and Biological Evaluation of Some Novel Pyrrolizine Derivatives as COX Inhibitors with Anti-Inflammatory/Analgesic Activities and Low Ulcerogenic Liability, Molecules. 21 (2016). doi:10.3390/molecules21020201.
49. R. Yang, C. Guo, Discovery of potent pyruvate dehydrogenase kinase inhibitors and evaluation of their anti-lung cancer activity under hypoxia, Med. Chem. Comm. 9 (2018) 1843–1849. doi:10.1039/c8md00453f.
50. B. Schittek, T. Sinnberg, Biological functions of casein kinase 1 isoforms and putative roles in tumorigenesis, Mol. Cancer. 13 (2014) 231. doi:10.1186/1476-4598-13-231.
51. C. Talarico, V. Dattilo, L. D'Antona, M. Menniti, C. Bianco, F. Ortuso, S. Alcaro, S. Schenone, N. Perrotti, R. Amato, SGK1, the New Player in the Game of Resistance: Chemo-Radio Molecular Target and Strategy for Inhibition, Cell. Physiol. Biochem. 39 (2016) 1863–1876. doi:10.1159/000447885.
52. Y. Wang, Y. Chen, X. Cheng, K. Zhang, H. Wang, B. Liu, J. Wang, Design, synthesis and biological evaluation of pyrimidine derivatives as novel CDK2 inhibitors that induce apoptosis and cell cycle arrest in breast cancer cells, Bioorg. Med. Chem. 26 (2018) 3491–3501. doi:https://doi.org/10.1016/j.bmc.2018.05.024.
53. A.M. Gouda, E.A. Beshr, F.A. Almalki, H. Hisham, B. Fawzi Taj, A. Faiz Alnafaei, R. Sulaiman Alharazi, W. Mahmood kazi, M.S. Halawah, Arylpropionic acid-derived NSAIDs: New insights on derivatization, anticancer activity and potential mechanism of action, Bioorg. Chem. (2019) 103224. doi:https://doi.org/10.1016/j.bioorg.2019.103224.
54. G.M. Morris, R. Huey, W. Lindstrom, M.F. Sanner, R.K. Belew, D.S. Goodsell, A.J. Olson, AutoDock4 and AutoDockTools4: Automated docking with selective receptor flexibility, J. Comput. Chem. 30 (2009) 2785–2791. doi:10.1002/jcc.21256.

55. Dassault systems BIOVIA, Discovery Studio Visualizer, v16.1.0.15350, San Diego: Dassault systems, (2016).
56. B.S. Selinsky, K. Gupta, C.T. Sharkey, P.J. Loll, Structural analysis of NSAID binding by prostaglandin H2 synthase: time-dependent and time-independent inhibitors elicit identical enzyme conformations, Biochemistry. 40 (2001) 5172–5180. doi:10.1021/bi010045s.
57. A.M. Gouda, F.A. Almalki, Carprofen : a theoretical mechanistic study to investigate the impact of hydrophobic interactions of alkyl groups on modulation of COX - 1/2 binding selectivity, SN Appl. Sci. 1 (2019). https://doi.org/10.1007/s42452-019-0335-5.
58. F.A. Almalki, A.M. Gouda, M.H. Bin Ali, O.M. Almehmadi, Profens: a comparative molecular docking study into cyclooxygenase-1/2, Drug Invent Today 11 (2019) 480–487.
59. R.G. Kurumbail, A.M. Stevens, J.K. Gierse, J.J. McDonald, R.A. Stegeman, J.Y. Pak, D. Gildehaus, J.M. Miyashiro, T.D. Penning, K. Seibert, P.C. Isakson, W.C. Stallings, Structural basis for selective inhibition of cyclooxygenase-2 by anti-inflammatory agents, Nature. 384 (1996) 644–648. doi:10.1038/384644a0.
60. K.S. Bhullar, N.O. Lagaron, E.M. McGowan, I. Parmar, A. Jha, B.P. Hubbard, H.P.V. Rupasinghe, Kinase-targeted cancer therapies: progress, challenges and future directions, Mol. Cancer. 17 (2018) 48. doi:10.1186/s12943-018-0804-2.
61. S. Baumli, A.J. Hole, M.E.M. Noble, J.A. Endicott, The CDK9 C-helix exhibits conformational plasticity that may explain the selectivity of CAN508, ACS Chem. Biol. 7 (2012) 811–816. doi:10.1021/cb2004516.
62. B. Zhao, A. Smallwood, J. Yang, K. Koretke, K. Nurse, A. Calamari, R.B. Kirkpatrick, Z. Lai, Modulation of kinase-inhibitor interactions by auxiliary protein binding: crystallography studies on Aurora A interactions with VX-680 and with TPX2, Protein Sci. 17 (2008) 1791–1797. doi:10.1110/ps.036590.108.
63. Z. Karoulia, Y. Wu, T.A. Ahmed, Q. Xin, J. Bollard, C. Krepler, X. Wu, C. Zhang, G. Bollag, M. Herlyn, J.A. Fagin, A. Lujambio, E. Gavathiotis, P.I. Poulikakos, An Integrated Model of RAF Inhibitor Action Predicts Inhibitor Activity against Oncogenic BRAF Signaling, Cancer Cell. 30 (2016) 485–498. doi:10.1016/j.ccell.2016.06.024.
64. J. Stamos, M.X. Sliwkowski, C. Eigenbrot, Structure of the epidermal growth factor receptor kinase domain alone and in complex with a 4-anilinoquinazoline inhibitor, J. Biol. Chem. 277 (2002) 46265–46272. doi:10.1074/jbc.M207135200.

65. R.A. Laskowski, M.B. Swindells, LigPlot+: multiple ligand-protein interaction diagrams for drug discovery, J. Chem. Inf. Model. 51 (2011) 2778–2786. doi:10.1021/ci200227u.

Declaration of interests

☒ The authors declare that they have no known competing financial interests or personal relationships that could have appeared to influence the work reported in this paper.

☐The authors declare the following financial interests/personal relationships which may be considered as potential competing interests: